

Transverse momentum dependent factorisation in the target fragmentation region at small x

Paul Caucal^{1,*} and Farid Salazar^{2,3,4,5,†}

¹*SUBATECH UMR 6457 (IMT Atlantique, Université de Nantes, IN2P3/CNRS), 4 rue Alfred Kastler, 44307 Nantes, France*

²*Department of Physics, Temple University, Philadelphia, PA 19122 - 1801, USA*

³*RIKEN-BNL Research Center, Brookhaven National Laboratory, Upton, New York 11973, USA*

⁴*Physics Department, Brookhaven National Laboratory, Upton, New York 11973, USA*

⁵*Institute for Nuclear Theory, University of Washington, Seattle WA 98195-1550, USA*

We consider the differential cross-section for single-inclusive jet production with transverse momentum P_\perp in Deep Inelastic Scattering (DIS) at small Bjorken x_{Bj} , mediated by a virtual photon with virtuality Q^2 . Unlike most studies at small x , which focus on particle production in the current fragmentation region, we investigate the kinematic regime where the jet is produced in the target fragmentation hemisphere of the Breit frame, and with $P_\perp \ll Q$. For a longitudinally polarised photon, we demonstrate that this cross-section is not power suppressed in P_\perp/Q and we derive a factorised expression in terms of transverse momentum dependent (TMD) quark and gluon fracture functions. Our formula, valid at next-to-leading order in α_s at small x , is akin to the Altarelli-Martinelli identity for the longitudinal DIS structure function. Numerical estimates show that the quark TMD fracture function is the most sensitive to saturation effects in large nuclei.

Transverse momentum dependent (TMD) distribution functions [1], which characterise the distribution of quarks and gluons inside nuclei in terms of their longitudinal and transverse momenta with respect to the nucleus direction of motion, provide fundamental insight on hadron substructure bounded in nuclei. As such, their measurement is one of the main goals of the Electron-Ion Collider (EIC) scientific program [2–4]. A key process to measure the quark TMDs is semi-inclusive hadron production in Deep Inelastic Scattering (DIS) in the regime where the transverse momentum squared P_\perp^2 of the hadron (measured in the Breit frame [5–7]) is much smaller than the virtuality Q^2 of the photon probing the target wavefunction [8–10].

Most studies of semi-inclusive DIS (SIDIS) in the TMD literature have focused on hadrons measured in the current (i.e. virtual photon) fragmentation region of the Breit frame for which a factorisation theorem has been established at leading power (LP) in P_\perp/Q [11–13]. On the other hand, the case where the hadron is measured in the target fragmentation hemisphere has received less attention, although the corresponding cross-section in the Bjorken limit (fixed Bjorken variable $x_{\text{Bj}} \lesssim 1$, large Q^2) admits a factorisation theorem [14, 15] formulated in terms of TMD fracture functions [16–20]. These TMD fracture functions describe the distribution of partons in the target probed by the virtual photon under the condition that a spectator parton fragments into a hadron in the target hemisphere, and thus carry complementary information on the internal parton dynamics [21].

In this paper, we investigate for the first time jet production in SIDIS in the target fragmentation region in the Regge limit [22], i.e. small $x_{\text{Bj}} \ll 1$ at fixed Q^2 . Our study is also motivated by the connection [23] between fracture functions and nucleon energy-energy correlators [24], a novel observable proposed to search for sat-

uration effects at small x [25]. For the sake of simplicity, we consider the longitudinally polarised photon contribution. An analogous analysis can be carried out for the transversely polarized case. Surprisingly, unlike hadron/jet measured in the current hemisphere, which give power suppressed contributions to the longitudinal structure function [9, 26–29], we demonstrate here (i) that the single-inclusive jet cross-section in SIDIS mediated by a longitudinally polarised photon is LP (i.e. not suppressed by P_\perp/Q for $Q \gg P_\perp$ starting from next-to-leading order (NLO) in α_s , and controlled by jets produced in the target fragmentation region, (ii) that this LP contribution factorises in terms of TMD quark and gluon fracture functions [30] for which we give explicit analytic expressions in the saturation regime $P_\perp \sim Q_s$ with Q_s the nucleus saturation scale.

Our strategy to achieve this is simple: we shall extract the LP contribution to the single-inclusive jet cross-section in longitudinally polarised DIS based on the NLO formula *valid for general jet kinematics* at small x . A byproduct of this calculation will be the proof that the LP term in the P_\perp/Q expansion comes indeed from jets produced in the target hemisphere. The benefit of using jets is to avoid non perturbative inputs like final state fragmentation functions [31, 32], although the phase space for producing jets with large enough P_\perp while being in the regime $P_\perp \ll Q, x_{\text{Bj}} \ll 1$ is quite narrow at the EIC (the situation will be more favourable at future high energy e^-p/A colliders [33–36]).

We first introduce the SIDIS jet cross-section, in the one virtual photon ($\gamma_{T/L}^*$) exchange approximation [26],

$$\frac{d\sigma^{e^-+A \rightarrow e^-'+\text{jet}+X}}{dx_{\text{Bj}}dQ^2d^2\mathbf{P}_\perp} = \sum_i \sigma_{0,i}^{\text{DIS}} [F_{UU,T} + \varepsilon F_{UU,L}], \quad (1)$$

where $\sigma_{0,i}^{\text{DIS}} = 4\pi\alpha_{\text{em}}^2 e_i^2 (1-y+y^2/2)/(x_{\text{Bj}}Q^4)$ is the Born level hard factor and $\varepsilon = (1-y)/(1-y+y^2/2)$ is the ratio

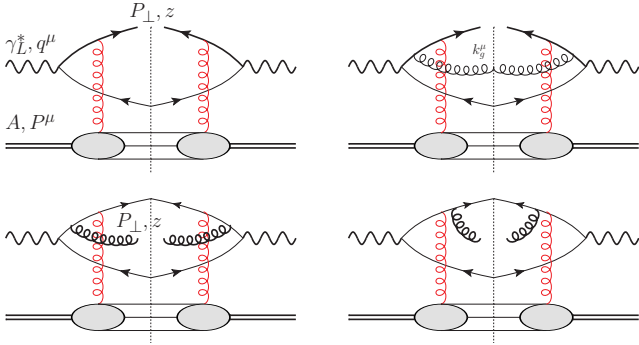


Figure 1. Feynman graphs for the $\gamma_L^* + A \rightarrow \text{jet} + X$ sub-process at small x_{Bj} . Top: LO (left) and LP NLO diagram (right) for a quark jet measurement. Bottom: examples of LP NLO diagrams for gluon jet production. $q \leftrightarrow \bar{q}$ exchanged and interference graphs are not displayed but contribute at LP.

between the longitudinal and transverse photon fluxes. Q^2 , x_{Bj} and $y = Q^2/(sx_{\text{Bj}})$ respectively denote the virtuality, the Bjorken variable, and the inelasticity for a fixed $e^- + A$ center-of-mass energy per nucleon \sqrt{s} . α_{em} is the fine structure constant and e_i is the fractional electric charge of the light quark of flavour i . $F_{UU,T}$ and $F_{UU,L}$ are respectively the transverse and longitudinal contributions to the SIDIS jet cross-section. In the limit $P_\perp \ll Q$, $F_{UU,T}$ is leading-twist at tree-level and the cross-section for transversely polarised γ_T^* admits TMD factorisation; the NLO calculation of $F_{UU,T}$ for jets at moderate x_{Bj} can be found in [37]. We will not discuss other TMDs arising when considering polarised beams or the azimuth of \mathbf{P}_\perp w.r.t. the electron plane [9, 26].

As a proof of principle, we shall compute $F_{UU,L}(x_{\text{Bj}}, Q^2, \mathbf{P}_\perp)$ in Eq. (1) in the small x_{Bj} limit. This is sufficient to prove that $F_{UU,L}$ is LP. The calculation at small x_{Bj} is performed in the Colour Glass Condensate (CGC) effective field theory [38–42] and in the dipole frame [43–46] where the virtual photon has 4-momentum $q^\mu = (q^+, -Q^2/(2q^+), \mathbf{0}_\perp)$ and a nucleon from the nucleus A has 4-momentum $P^\mu = (0, P^-, \mathbf{0}_\perp)$ in light-cone coordinates [47]. Another advantage of the small x limit is that the CGC provides an input for the non-perturbative part for the quark and gluon TMD parton distribution functions (PDF) [48–54]. This is also the case for TMD fracture functions. In particular, our calculation shall provide for the first time the CGC expressions for the TMD fracture functions at small x .

The LO cross-section is given by the top-left diagram in Fig. 1, where the measured quark-jet with four-momentum k^μ has a longitudinal momentum fraction $z = k \cdot P / (P \cdot q) = k^+ / q^+$ and transverse momentum \mathbf{P}_\perp w.r.t. the photon direction. In this diagram, multiple scattering of the quark-antiquark colour dipole with transverse size \mathbf{r}_{xy} off the shockwave — pictured by a red gluon in Fig. 1 and representing the dense gluon

field of the target — is encoded into the dipole S -matrix

$$\mathcal{D}_F(x, \mathbf{q}_\perp) \equiv \int_{\mathbf{r}_{xy}} \frac{e^{-i\mathbf{q}_\perp \cdot \mathbf{r}_{xy}}}{(2\pi)^2} \frac{1}{N_c} \langle \text{Tr} [V_{\mathbf{x}_\perp} V_{\mathbf{y}_\perp}^\dagger] \rangle_x, \quad (2)$$

with $V_{\mathbf{x}_\perp}$ a light-like Wilson with transverse coordinate $\mathbf{x}_\perp = \mathbf{B}_\perp + \mathbf{r}_{xy}/2$ in the fundamental representation of $SU(3)$ describing the colour precession of the quark while eikonal interacting with the target field at \mathbf{x}_\perp (resp. $\mathbf{y}_\perp = \mathbf{B}_\perp - \mathbf{r}_{xy}/2$ for the antiquark). We use the shorthand notation $\int_{\mathbf{r}_{xy}} = \int d^2\mathbf{r}_{xy}$. The dependence upon the impact parameter \mathbf{B}_\perp of the dipole in Eq. (2) is omitted. The x dependence of the CGC average $\langle \dots \rangle_x$ over gluon field configurations is determined by the BK-JIMWLK evolution equation [55–63] or by its linear version corresponding to the BFKL equation [64, 65] in the limit $q_\perp \gg Q_s$, with Q_s the nucleus saturation scale. Ultimately, x is fixed by four-momentum conservation at the scale $x = x_{\text{Bj}}$. Gathering the dipole S -matrix and the hard factor \mathcal{H}_{LO} for producing the $q\bar{q}$ pair from the virtual photon, we get [50, 66]

$$F_{UU,L}^{\text{LO}} = \frac{N_c}{2\pi^4} \int_{\mathbf{B}_\perp, \mathbf{q}_\perp} \mathcal{D}_F(x, \mathbf{q}_\perp) \int_0^1 dz |\mathcal{H}_{\text{LO}}|^2, \quad (3)$$

with

$$\mathcal{H}_{\text{LO}} = \frac{\bar{Q}^2}{(\mathbf{P}_\perp - \mathbf{q}_\perp)^2 + \bar{Q}^2} - \frac{\bar{Q}^2}{P_\perp^2 + \bar{Q}^2}, \quad (4)$$

and $\bar{Q}^2 = z(1-z)Q^2$. At this stage, Eq. (3) contains all kinematic $\mathcal{O}(P_\perp/Q)$ and saturation $\mathcal{O}(Q_s/Q)$ power corrections at small x [67]. Performing the integral over z and expanding the result in the limit $Q \gg P_\perp$ yields

$$F_{UU,L}^{\text{LO}, \text{N}^2\text{LP}} = \frac{N_c P_\perp^2}{\pi^4 Q^2} \int_{\mathbf{B}_\perp, \mathbf{q}_\perp} \mathcal{D}_F(x, \mathbf{q}_\perp) \left[\frac{(\mathbf{P}_\perp - \mathbf{q}_\perp)^2}{P_\perp^2} + 1 - \frac{2(\mathbf{P}_\perp - \mathbf{q}_\perp)^2}{P_\perp^2 - (\mathbf{P}_\perp - \mathbf{q}_\perp)^2} \ln \left(\frac{P_\perp^2}{(\mathbf{P}_\perp - \mathbf{q}_\perp)^2} \right) \right]. \quad (5)$$

In this limit, the integral over z in Eq. (3) is dominated by the two endpoints $z = 0$ and $z = 1$, that is by the so-called aligned jet configurations [37, 50, 52, 66] where the produced $q\bar{q}$ pair is highly asymmetric in longitudinal space with either $z \sim P_\perp^2/Q^2$ or $1-z \sim P_\perp^2/Q^2$. As clear from this result, the LO $F_{UU,L}$ is next-to-next-to-leading power (N²LP) since it is suppressed by P_\perp^2/Q^2 and Eq. (5) provides an explicit expression from first QCD principles of the LO and N²LP contribution to $F_{UU,L}$ at small x_{Bj} (see also [68, 69]).

Physically, a longitudinally polarised photon cannot directly couple to a (sea) quark at LO from the target because of helicity conservation [70, 71]. The same argument applies for the longitudinal structure function $F_L(x, Q^2)$ which also vanishes at LO in the naive parton model by virtue of the Callan-Gross relation [70]. That said, we note in anticipation of a future discussion that the integral over \mathbf{P}_\perp of $F_{UU,L}^{\text{LO}}$ in

Eq. (3) nevertheless contributes to F_L at LP such that $F_L^{\text{LO}} = \alpha_s/(3\pi) xg(x, Q^2)$ [72–75] (cf. Supplemental Material [76]), where the gluon PDF is defined, for $x \ll 1$, as [50, 53, 77, 78]

$$xg(x, Q^2) \equiv \int^{Q^2} d^2 \mathbf{q}_\perp \int_{\mathbf{B}_\perp} \frac{N_c}{2\pi^2 \alpha_s} q_\perp^2 \mathcal{D}_F(x, \mathbf{q}_\perp). \quad (6)$$

We now consider the NLO correction to Eq. (3). The complete NLO correction at small x_{Bj} to the SIDIS jet cross-section for longitudinally polarised virtual photon has been computed in [79, 80] (see also [81–83]). We shall focus on the top right real diagram in Fig. 1, labelled $R1 \times R1^*$, where the quark-jet P_\perp is measured (the case where the antiquark jet is tagged is identical). This diagram contributes to $F_{UU,L}$ as (cf. Eq. (3.33) in [80]),

$$\begin{aligned} F_{UU,L}^{R1 \times R1^*} &= \frac{\alpha_s N_c}{8\pi^8} \int_{\mathbf{x}_\perp, \mathbf{x}'_\perp, \mathbf{y}_\perp, \mathbf{z}_\perp} e^{-i\mathbf{P}_\perp \cdot \mathbf{r}_{x'x'}} \int_0^1 dz \\ &\times \int_0^{1-z} \frac{dz_g}{z_g} \left(1 - \frac{z_g}{1-z}\right)^2 \bar{Q}^4 K_0(QX_R) K_0(QX'_R) \\ &\times \frac{\mathbf{r}_{zx} \cdot \mathbf{r}_{zx'}}{r_{zx}^2 r_{zx'}^2} \left(1 + \frac{z_g}{z} + \frac{z_g^2}{2z^2}\right) \Xi(\mathbf{x}_\perp, \mathbf{y}_\perp, \mathbf{z}_\perp, \mathbf{x}'_\perp), \quad (7) \end{aligned}$$

with $\mathbf{r}_{ab} \equiv \mathbf{a}_\perp - \mathbf{b}_\perp$. Here $z_g = k_g \cdot P / (P \cdot q)$ is the longitudinal momentum fraction of the gluon with 4-momentum k_g^μ and \mathbf{z}_\perp its transverse coordinate when it eikonally crosses the shockwave. The integral over z_g is divergent as $z_g \rightarrow 0$, yet as we shall see, the high virtuality limit of Eq. (7) is insensitive to this rapidity divergence [84]. Further, K_0 is the zeroth order modified Bessel function entering into the $q\bar{q}g$ light-cone wave-function with the effective $q\bar{q}g$ size given by $X_R^2 = z(1-z-z_g)r_{xy}^2 + z z_g r_{zx}^2 + (1-z-z_g)z_g r_{zy}^2$ and likewise for X'_R with the replacement $\mathbf{r}_{xy} \rightarrow \mathbf{r}_{x'y}$. Last, the CGC correlator Ξ associated with the eikonal interaction of the $q\bar{q}g$ system with the target gluon field reads

$$\begin{aligned} \Xi &= \frac{N_c}{2} \langle D_{xx'} - D_{xz} D_{zy} - D_{yz} D_{zx'} + 1 \rangle_x \\ &- \frac{1}{2N_c} \langle D_{xx'} - D_{xy} - D_{yx'} + 1 \rangle_x, \quad (8) \end{aligned}$$

with the shorthand notation $D_{xy} = \text{Tr}(V_{\mathbf{x}_\perp} V_{\mathbf{y}_\perp}^\dagger) / N_c$.

We would like to demonstrate that Eq. (7) has a leading twist component in the limit $Q^2 \gg P_\perp^2$. As previously mentioned, this limit is dominated by aligned jet configurations, yet for this diagram, the end-point $z = 1$ is power suppressed because of the upper limit of the z_g integral coming from longitudinal momentum conservation. Let us then focus on the endpoint $z = 0$ with the scaling $z \sim P_\perp^2 / Q^2 \ll 1$. In this regime, the term given by $z_g^2 / (2z^2)$ in the third line of Eq. (7) dominates. The additional power of z_g^2 cancels the light-cone divergence in $1/z_g$ of the z_g integral such that one can safely integrate over z_g between 0 and 1, with typically $z_g \sim 1/2$.

Furthermore, the hierarchy of scales $Q \gg P_\perp$ must be reflected in a hierarchy of transverse distances among the $q\bar{q}g$ system while interacting with the shockwave. From the phase in Eq. (7), we have $r_{xx'} \sim 1/P_\perp$ (and likewise for r_{xy} and $r_{x'y}$ since $\mathbf{r}_{xx'} = \mathbf{r}_{xy} - \mathbf{r}_{x'y}$) such that the $q\bar{q}$ pair is widely separated in the amplitude and complex conjugate amplitude. Moreover, the $q\bar{q}g$ pair must have a small size as the condition $X_R \lesssim 1/Q$ from the K_0 Bessel function implies $r_{zy} \sim 1/Q$. We can therefore approximate $X_R \approx z r_{xy}^2 + z_g(1-z_g)r_{zy}^2$ (and likewise for X'_R) where it is now easy to verify that both terms in X_R are of the same order. Similarly, the Weizsäcker–Williams gluon emission kernel $\mathbf{r}_{zx}^i / r_{zx}^2$ in Eq. (7) is approximated by $-\mathbf{r}_{xy}^i / r_{xy}^2$. Finally, using $\mathbf{z}_\perp \sim \mathbf{y}_\perp$, the CGC correlator Eq. (8) simplifies into a sum of dipoles, with an overall C_F Casimir factor:

$$\Xi \approx C_F \langle D_{xx'} - D_{xy} - D_{yx'} + 1 \rangle_x, \quad (9)$$

$$= C_F \int_{\mathbf{q}_\perp} (e^{i\mathbf{q}_\perp \cdot \mathbf{r}_{xy}} - 1) (e^{-i\mathbf{q}_\perp \cdot \mathbf{r}_{x'y}} - 1) \mathcal{D}_F(x, \mathbf{q}_\perp). \quad (10)$$

Under these approximations, one can analytically perform the transverse coordinate integrals in Eq. (7), and extract the $Q \gg P_\perp$ limit of the final z integration (cf. Supplemental Material), such that

$$\begin{aligned} F_{UU,L}^{\text{NLO,LP-}q} &= \frac{\alpha_s C_F}{2\pi} \times \frac{N_c}{4\pi^4} \int_{\mathbf{B}_\perp, \mathbf{q}_\perp} \mathcal{D}_F(x, \mathbf{q}_\perp) \\ &\times \left[1 - \frac{\mathbf{P}_\perp \cdot (\mathbf{P}_\perp - \mathbf{q}_\perp)}{P_\perp^2 - (\mathbf{P}_\perp - \mathbf{q}_\perp)^2} \ln \left(\frac{P_\perp^2}{(\mathbf{P}_\perp - \mathbf{q}_\perp)^2} \right) \right], \quad (11) \end{aligned}$$

which is the complete NLO result at LP and small x for the quark-jet contribution to $F_{UU,L}$ (using similar arguments, one shows that other diagrams not displayed in Fig. 1 are not LP). This expression neglects power corrections in P_\perp/Q , but it resums to all orders saturation power corrections in Q_s/P_\perp . It can then be used also in the saturation regime $P_\perp \sim Q_s$ so long as $P_\perp, Q_s \ll Q$.

Most importantly, the NLO correction to $F_{UU,L}$ is leading twist; unlike Eq. (5), it is not suppressed by P_\perp/Q . The mathematical derivation gives physical insight on why it is so: the leading twist component comes from the regime $z \sim P_\perp^2 / Q^2 \ll 1$, meaning that in the Breit frame where the jet rapidity reads $\eta = \ln(zQ/P_\perp) \sim \ln(P_\perp/Q) < 0$, the jet is produced in the target fragmentation hemisphere (cf Fig 2-left) and not in the current (or γ^*) fragmentation one where the leading hadron is measured in hadronic SIDIS and where the corresponding TMD factorisation theorem holds [13, 27, 29, 85]. From a physical standpoint, the condition $z \sim P_\perp^2 / Q^2$ can be understood as follows: to bypass the LO helicity conservation argument, a real gluon must be emitted with enough longitudinal phase space. Then, the LP contribution comes from the aligned jet configuration with either $z \sim 1$ or $z \sim P_\perp^2 / Q^2$. However, the former is forbidden by longitudinal momentum conservation imposing $z_g \leq 1 - z$ for real gluons.

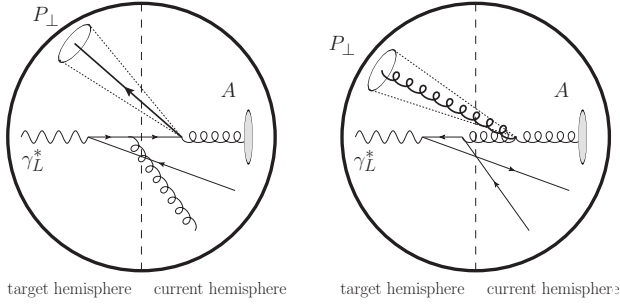


Figure 2. Breit frame views of the LP jet produced in $\gamma_L^* + A$ collision at small x in the quark (left) and gluon (right) production channels.

In Eq. (11), the expression after the \times symbol must be interpreted as the LO quark TMD fracture function $x\mathcal{F}_q$:

$$x\mathcal{F}_q(x, \mathbf{P}_\perp) = \frac{N_c}{4\pi^4} \int_{\mathbf{B}_\perp, \mathbf{q}_\perp} \mathcal{D}_F(x, \mathbf{q}_\perp) \times \left[1 - \frac{\mathbf{P}_\perp \cdot (\mathbf{P}_\perp - \mathbf{q}_\perp)}{P_\perp^2 - (\mathbf{P}_\perp - \mathbf{q}_\perp)^2} \ln \left(\frac{P_\perp^2}{(\mathbf{P}_\perp - \mathbf{q}_\perp)^2} \right) \right]. \quad (12)$$

It turns out to be identical, at this α_s order, to the standard TMD sea quark distribution function probed in small x SIDIS mediated by a transversely polarised photon in the current fragmentation region [48–52, 86], including in the saturation regime $P_\perp \sim Q_s$. This is non

trivial as the longitudinal photon does not directly couple to sea quarks in the target, as illustrated in Fig. 2-left.

In addition to the diagrams where the fermionic jet is tagged, there are LP NLO contributions to the SIDIS jet cross-section where the gluon jet with transverse momentum $\mathbf{P}_\perp = \mathbf{k}_{g\perp}$ and $z = z_g \lesssim P_\perp^2/Q^2$ is measured (examples of diagrams are shown in the second row of Fig. 1). They are computed in detail in the Supplemental Material following the method outlined above. Remarkably, the leading twist component of these diagrams now depends on the gluon-gluon dipole S -matrix,

$$\mathcal{D}_A(x, \mathbf{q}_\perp) \equiv \int_{r_{zz'}} \frac{e^{-i\mathbf{q}_\perp \cdot \mathbf{r}_{zz'}}}{(2\pi)^2 (N_c^2 - 1)} \left\langle U_{z_\perp}^{ab} U_{z'_\perp}^{\dagger, ba} \right\rangle_x, \quad (13)$$

with U_{z_\perp} a Wilson line in the *adjoint* representation. Indeed, in the limit $Q \gg P_\perp$ with P_\perp now that of the gluon, the $q\bar{q}$ pair becomes the smallest dipole with transverse size $r_{xy} \sim 1/Q$ much smaller than the transverse distance $r_{zx} \sim 1/P_\perp$ between the $q\bar{q}$ pair and the gluon. Like in semi-inclusive diffractive DIS [87, 88], an effective gluon-gluon dipole is built in the amplitude out of the NLO gluon and this very small $q\bar{q}$ dipole. The gluon-jet contribution eventually reads

$$F_{UU,L}^{\text{NLO,LP-g}} = \frac{\alpha_s}{3\pi} \times x\mathcal{F}_g(x, \mathbf{P}_\perp), \quad (14)$$

with the gluon TMD fracture function $x\mathcal{F}_g$ at small x :

$$x\mathcal{F}_g(x, \mathbf{P}_\perp) = \frac{N_c^2 - 1}{4\pi^4} \int_{\mathbf{B}_\perp, \mathbf{q}_\perp} \mathcal{D}_A(x, \mathbf{q}_\perp) \times \left\{ \ln \left(\frac{1}{x} \right) \frac{q_\perp^2}{P_\perp^2} - 1 - \frac{(\mathbf{P}_\perp - \mathbf{q}_\perp)^2 - q_\perp^2}{2P_\perp^2} \ln \left(\frac{(\mathbf{P}_\perp - \mathbf{q}_\perp)^2}{P_\perp^2} \right) + \left(1 - \frac{2(\mathbf{P}_\perp \cdot (\mathbf{P}_\perp - \mathbf{q}_\perp))^2}{P_\perp^2 (\mathbf{P}_\perp - \mathbf{q}_\perp)^2} \right) \frac{(\mathbf{P}_\perp - \mathbf{q}_\perp)^2}{P_\perp^2 - (\mathbf{P}_\perp - \mathbf{q}_\perp)^2} \ln \left(\frac{(\mathbf{P}_\perp - \mathbf{q}_\perp)^2}{P_\perp^2} \right) \right\}. \quad (15)$$

As a cross-check of Eq. (15), we consider the dilute limit $P_\perp \gg q_\perp \sim Q_s$. It is easy to check that, up to power corrections in Q_s^4/P_\perp^4 , we have

$$x\mathcal{F}_g(x, \mathbf{P}_\perp) \approx \frac{\alpha_s}{2\pi^2} \frac{1}{P_\perp^2} \int_x^1 d\xi P_{gg}(\xi) xg(x, P_\perp^2), \quad (16)$$

with $P_{gg}(\xi) = 2N_c(1 - \xi(1 - \xi))^2/[\xi(1 - \xi)_+]$ the $g \rightarrow gg$ splitting function. Thus, the gluon TMD in Eq. (15) can be interpreted [89, 90] as the convolution between the (adjoint) dipole gluon TMD \mathcal{D}_A sourcing the parent gluon from the target wave-function and a TMD $g \rightarrow gg$ splitting function [91], where one daughter gluon gives the measured jet while the other interacts with the virtual photon via a $q\bar{q}$ pair, as shown in Fig. 2-right.

Gathering the fermion and gluon jet contributions, our final result for the single-inclusive jet cross-section

in longitudinally polarised DIS at LP and small x is

$$F_{UU,L}^{\text{LP}} = \frac{\alpha_s C_F}{2\pi} \sum_{k=q,\bar{q}} x\mathcal{F}_k(x, \mathbf{P}_\perp) + \frac{\alpha_s}{3\pi} x\mathcal{F}_g(x, \mathbf{P}_\perp). \quad (17)$$

Eq. (17), together with Eqs. (12)-(15), are the main results of this paper. Eq. (17) is analogous to the Altarelli-Martinelli identity [92, 93] for F_L at one loop in the collinear factorisation α_s power counting:

$$F_L = \frac{\alpha_s x^2}{2\pi} \int_x^1 \frac{dz}{z^3} \left[\frac{8}{3} F_2(z, Q^2) + 4 \left(1 - \frac{x}{z} \right) zg(z, Q^2) \right] \approx \frac{\alpha_s C_F}{2\pi} (xq(x, Q^2) + x\bar{q}(x, Q^2)) + \frac{\alpha_s}{3\pi} xg(x, Q^2), \quad (18)$$

where we have used $F_2 = xq + x\bar{q}$ in the LO naive parton model. Yet, it differs from the latter in two crucial aspects: (i) Eq. (17) is valid at the TMD level (\mathbf{P}_\perp unintegrated), (ii) it is a two loop result in the collinear

factorisation α_s power counting since $x\mathcal{F}_{q/g} = \mathcal{O}(\alpha_s)$. This result also agrees with the small x limit of Eq. (4.2) in [94] where $F_{UU,L}$ is computed at NLO in the Bjorken limit for hadrons produced in the target hemisphere.

Integrating Eq. (17) for $P_\perp \leq Q$ gives the one loop correction to F_L at small x and leading twist. Albeit $\mathcal{O}(\alpha_s^2)$, the result has the same structure as Eq. (18) with the quark PDF xq at small x defined as [37, 90, 95, 96]

$$xq(x, Q^2) = \int^{Q^2} d^2\mathbf{P}_\perp x\mathcal{F}_q(x, \mathbf{P}_\perp), \quad (19)$$

and likewise for $x\bar{q}$. In the gluon channel, $xg(x, Q^2)$ is now defined by the \mathbf{P}_\perp -integral of Eq. (15). This integral is controlled by the perturbative $1/P_\perp^2$ tail obtained in Eq. (16) and gives what one expects: the $x \rightarrow 0$ limit of one DGLAP step of the LO gluon PDF defined in Eq. (6). In the end, Eq. (17) shows that the Altarelli-Martinelli relation in NLO collinear factorisation actually works at two loops in the $x \rightarrow 0$ limit.

We finally conclude with a numerical study of the TMD fracture functions at small x . Our goal is to illustrate the P_\perp dependence of $x\mathcal{F}_{q/g}$ and to assess the importance of gluon saturation. To compute the dipole S -matrix in momentum space, we use the McLerran-Venugopalan model [97, 98] for a nucleus with atomic mass number A ,

$$\langle D_{xy} \rangle = \exp \left[-\frac{1}{4} A^{1/3} Q_{s,p}^2 r_{xy}^2 \ln \left(\frac{1}{r_{xy}\Lambda} + e \right) \right], \quad (20)$$

with parameters $Q_{s,p}^2 = 0.2 \text{ GeV}^2$ for the bare proton saturation scale at $x = 0.01$, $\Lambda = 0.24 \text{ GeV}$ [99, 100]. Thanks to the $+e$ term in the Coulomb logarithm, the Fourier transform $\mathcal{D}_F(x, \mathbf{q}_\perp)$ of Eq. (20) is positive-definite [101, 102]. To get the adjoint dipole in Eq. (13), we simply rescale $Q_{s,p}^2 \rightarrow N_c Q_{s,p}^2 / C_F$ in Eq. (20). These choices are meant to illustrate the general behaviour of $x\mathcal{F}_{q/g}$ with motivated values for the model parameters; we postpone phenomenological studies to future work.

In Fig. 3-top, the red and blue curves respectively correspond to the P_\perp -dependence of the quark and gluon TMD fracture functions, at LO in the small x limit, as given by Eqs. (12)-(15). They are represented for two values of the saturation scale corresponding to a proton (dashed curves) and a large nucleus with $A^{1/3} = 5$ (plain curves). The bottom plot displays the ratio of the quark and gluon TMD fracture functions between a large nucleus and a proton, normalised by $A^{-1/3}$.

The quark TMD fracture function has two regimes: at large P_\perp , one recognises the perturbative tail $\propto A^{1/3} Q_{s,p}^2 / P_\perp^2$, such that the ratio A/p in the bottom plot converges towards 1 for $P_\perp \gg Q_s$. For $P_\perp \ll Q_s$, the growth of the quark TMD saturates [48–50] and reaches the universal (independent of A) unitary limit.

On the other hand, the gluon TMD fracture function Eq. (15) shows very little sensitivity to saturation effect,

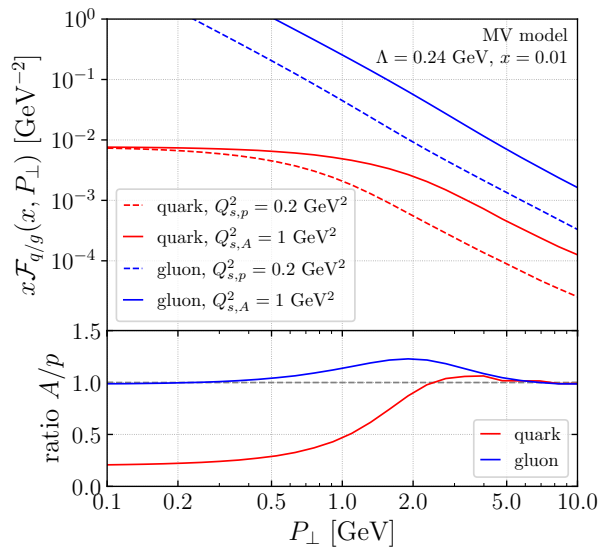


Figure 3. Small- x quark and gluon TMD fracture functions at LO for a proton and a nucleus with $A^{1/3} = 5$. Details in text.

since the $1/P_\perp^2$ perturbative tail extends down to values of P_\perp smaller than Q_s . The small impact of saturation is also manifest in the ratio plot, which is approximately constant except around $P_\perp \sim Q_s$. This is a consequence of the first term in the curly bracket of Eq. (15), which behaves like $1/P_\perp^2$ even for $P_\perp \ll Q_s$. This term is caused by final state gluon emissions in the dipole frame (bottom-right diagram in Fig. 1) which are insensitive to the scattering of the $q\bar{q}$ dipole off the shockwave. Obviously, the $1/P_\perp^2$ enhancement at small P_\perp will be suppressed by a Sudakov factor [103–110], as for the quark TMD [37, 111]. The computation of the Sudakov factor for Eq. (15) requires a two-loop calculation in the CGC.

That said, it is likely that the quark production channel will be the most sensitive to saturation effects, even after including the dominant higher order corrections via a Sudakov suppression factor, since such a factor would largely cancel in the A/p ratio [112]. One way to focus on quark-initiated jets produced in the target hemisphere would be to consider jets with open heavy flavour. We defer the computation of the quark mass corrections to Eq. (12) for a follow-up paper.

To summarise, we have unveiled a new contribution to TMD factorisation in SIDIS coming from jets produced in the target fragmentation region. We have derived a simple analytic expression for $F_{UU,L}$ at small x and leading twist in terms of TMD fracture functions, as shown in Eq. (17), opening a new way to explore saturation in and TMD phenomenology at the EIC. Our results also pave the way towards precision studies of nucleon energy-energy correlators [23, 25] at NLO. In the future, we plan to investigate diffractive fracture functions, as well as heavy flavour in the target region.

Acknowledgments. We would like to thank Edmond Iancu for useful remarks. Figures 1 and 2 have been created with JaxoDraw [113]. We are grateful for the support of the Saturated Glue (SURGE) Topical Theory Collaboration, funded by the U.S. Department of Energy, Office of Science, Office of Nuclear Physics. F.S. is also supported by the Laboratory Directed Research and Development of Brookhaven National Laboratory and RIKEN-BNL Research Center. Part of this work was conducted while F.S. was supported by the Institute for Nuclear Theory’s U.S. DOE under Grant No. DE-FG02-00ER41132. Finally, F.S. acknowledges support from the U.S. Department of Energy, Office of Science, Office of Nuclear Physics under the umbrella of the Quark-Gluon Tomography (QGT) Topical Collaboration with Award DE-SC0023646.

* caucal@subatech.in2p3.fr

† farid.salazar@temple.edu

- [1] R. Boussarie *et al.*, (2023), [arXiv:2304.03302 \[hep-ph\]](#).
- [2] A. Accardi *et al.*, *Eur. Phys. J. A* **52**, 268 (2016), [arXiv:1212.1701 \[nucl-ex\]](#).
- [3] R. Abdul Khalek *et al.*, *Nucl. Phys. A* **1026**, 122447 (2022), [arXiv:2103.05419 \[physics.ins-det\]](#).
- [4] P. Achenbach *et al.*, *Nucl. Phys. A* **1047**, 122874 (2024), [arXiv:2303.02579 \[hep-ph\]](#).
- [5] R. P. Feynman, *Photon-hadron interactions*, Frontiers in physics (Benjamin, Reading, 1972) pp. XVI, 282 pages.
- [6] K. H. Streng, T. F. Walsh, and P. M. Zerwas, *Z. Phys. C* **2**, 237 (1979).
- [7] J. A. Rinehimer and G. A. Miller, *Phys. Rev. C* **80**, 015201 (2009), [arXiv:0902.4286 \[nucl-th\]](#).
- [8] R. D. Tangerman and P. J. Mulders, *Phys. Rev. D* **51**, 3357 (1995), [arXiv:hep-ph/9403227](#).
- [9] P. J. Mulders and R. D. Tangerman, *Nucl. Phys. B* **461**, 197 (1996), [Erratum: *Nucl.Phys.B* 484, 538–540 (1997)], [arXiv:hep-ph/9510301](#).
- [10] D. Boer and P. J. Mulders, *Phys. Rev. D* **57**, 5780 (1998), [arXiv:hep-ph/9711485](#).
- [11] J. C. Collins, *Nucl. Phys. B* **396**, 161 (1993), [arXiv:hep-ph/9208213](#).
- [12] X.-d. Ji, J.-p. Ma, and F. Yuan, *Phys. Rev. D* **71**, 034005 (2005), [arXiv:hep-ph/0404183](#).
- [13] J. Collins, *Foundations of Perturbative QCD*, Cambridge Monographs on Particle Physics, Nuclear Physics and Cosmology, Vol. 32 (Cambridge University Press, 2023).
- [14] M. Grazzini, L. Trentadue, and G. Veneziano, *Nucl. Phys. B* **519**, 394 (1998), [arXiv:hep-ph/9709452](#).
- [15] J. C. Collins, *Phys. Rev. D* **57**, 3051 (1998), [Erratum: *Phys.Rev.D* 61, 019902 (2000)], [arXiv:hep-ph/9709499](#).
- [16] L. Trentadue and G. Veneziano, *Phys. Lett. B* **323**, 201 (1994).
- [17] D. Graudenz, *Nucl. Phys. B* **432**, 351 (1994), [arXiv:hep-ph/9406274](#).
- [18] D. de Florian and R. Sassot, *Phys. Rev. D* **56**, 426 (1997), [arXiv:hep-ph/9703228](#).
- [19] F. A. Ceccopieri and L. Trentadue, *Phys. Lett. B* **655**, 15 (2007), [arXiv:0705.2326 \[hep-ph\]](#).
- [20] M. Anselmino, V. Barone, and A. Kotzinian, *Phys. Lett. B* **699**, 108 (2011), [arXiv:1102.4214 \[hep-ph\]](#).
- [21] H. Avakian *et al.* (CLAS), *Phys. Rev. Lett.* **130**, 022501 (2023), [arXiv:2208.05086 \[hep-ex\]](#).
- [22] T. Regge, *Nuovo Cim.* **14**, 951 (1959).
- [23] K.-B. Chen, J.-P. Ma, and X.-B. Tong, *JHEP* **08**, 227 (2024), [arXiv:2406.08559 \[hep-ph\]](#).
- [24] X. Liu and H. X. Zhu, *Phys. Rev. Lett.* **130**, 091901 (2023), [arXiv:2209.02080 \[hep-ph\]](#).
- [25] H.-Y. Liu, X. Liu, J.-C. Pan, F. Yuan, and H. X. Zhu, *Phys. Rev. Lett.* **130**, 181901 (2023), [arXiv:2301.01788 \[hep-ph\]](#).
- [26] A. Bacchetta, M. Diehl, K. Goeke, A. Metz, P. J. Mulders, and M. Schlegel, *JHEP* **02**, 093 (2007), [arXiv:hep-ph/0611265](#).
- [27] A. Vladimirov, V. Moos, and I. Scimemi, *JHEP* **01**, 110 (2022), [arXiv:2109.09771 \[hep-ph\]](#).
- [28] S. Rodini and A. Vladimirov, *Phys. Rev. D* **110**, 034009 (2024), [arXiv:2306.09495 \[hep-ph\]](#).
- [29] M. A. Ebert, A. Gao, and I. W. Stewart, *JHEP* **06**, 007 (2022), [Erratum: *JHEP* 07, 096 (2023)], [arXiv:2112.07680 \[hep-ph\]](#).
- [30] Although we consider jet final states, we use the fracture function terminology as jet and leading hadron are essentially the same to the accuracy of interest.
- [31] A. Dumitru, A. Hayashigaki, and J. Jalilian-Marian, *Nucl. Phys. A* **765**, 464 (2006), [arXiv:hep-ph/0506308 \[hep-ph\]](#).
- [32] P. Caucal and F. Salazar, *JHEP* **12**, 130 (2024), [arXiv:2405.19404 \[hep-ph\]](#).
- [33] J. L. Abelleira Fernandez *et al.* (LHeC Study Group), *J. Phys. G* **39**, 075001 (2012), [arXiv:1206.2913 \[physics.acc-ph\]](#).
- [34] A. Abada *et al.* (FCC), *Eur. Phys. J. C* **79**, 474 (2019).
- [35] P. Agostini *et al.* (LHeC, FCC-he Study Group), *J. Phys. G* **48**, 110501 (2021), [arXiv:2007.14491 \[hep-ex\]](#).
- [36] O. Bruning, J. Jowett, M. Klein, D. Pellegrini, D. Schulte, and F. Zimmermann, *Future Circular Collider Study FCC-he Baseline Parameters*, Tech. Rep. (CERN, Geneva, 2017).
- [37] P. Caucal, E. Iancu, A. H. Mueller, and F. Yuan, (2024), [arXiv:2408.03129 \[hep-ph\]](#).
- [38] E. Iancu, A. Leonidov, and L. McLerran, in *Cargese Summer School on QCD Perspectives on Hot and Dense Matter* (2002) pp. 73–145, [arXiv:hep-ph/0202270](#).
- [39] E. Iancu and R. Venugopalan, “The Color glass condensate and high-energy scattering in QCD,” in *Quark-gluon plasma 4*, edited by R. C. Hwa and X.-N. Wang (2003) pp. 249–3363, [arXiv:hep-ph/0303204](#).
- [40] F. Gelis, E. Iancu, J. Jalilian-Marian, and R. Venugopalan, *Ann. Rev. Nucl. Part. Sci.* **60**, 463 (2010), [arXiv:1002.0333 \[hep-ph\]](#).
- [41] Y. V. Kovchegov and E. Levin, *Quantum Chromodynamics at High Energy*, Vol. 33 (Oxford University Press, 2013).
- [42] A. Morreale and F. Salazar, *Universe* **7**, 312 (2021), [arXiv:2108.08254 \[hep-ph\]](#).
- [43] B. Z. Kopeliovich, L. I. Lapidus, and A. B. Zamolodchikov, *JETP Lett.* **33**, 595 (1981).
- [44] G. Bertsch, S. J. Brodsky, A. S. Goldhaber, and J. F. Gunion, *Phys. Rev. Lett.* **47**, 297 (1981).
- [45] A. H. Mueller, *Nucl.Phys.* **B335**, 115 (1990).
- [46] N. N. Nikolaev and B. Zakharov, *Z.Phys.* **C49**, 607 (1991).
- [47] We neglect target mass corrections.
- [48] L. D. McLerran and R. Venugopalan, *Phys. Rev. D* **59**, 094002 (1999), [arXiv:hep-ph/9809427](#).
- [49] R. Venugopalan, *Acta Phys. Polon. B* **30**, 3731 (1999),

- arXiv:hep-ph/9911371.
- [50] A. H. Mueller, *Nucl. Phys. B* **558**, 285 (1999), arXiv:hep-ph/9904404.
- [51] B.-W. Xiao, F. Yuan, and J. Zhou, *Nucl. Phys. B* **921**, 104 (2017), arXiv:1703.06163 [hep-ph].
- [52] C. Marquet, B.-W. Xiao, and F. Yuan, *Phys. Lett. B* **682**, 207 (2009), arXiv:0906.1454 [hep-ph].
- [53] F. Dominguez, C. Marquet, B.-W. Xiao, and F. Yuan, *Phys. Rev. D* **83**, 105005 (2011), arXiv:1101.0715 [hep-ph].
- [54] E. Petreska, *Int. J. Mod. Phys. E* **27**, 1830003 (2018), arXiv:1804.04981 [hep-ph].
- [55] I. Balitsky, *Nucl. Phys. B* **463**, 99 (1996), arXiv:hep-ph/9509348.
- [56] Y. V. Kovchegov, *Phys. Rev. D* **60**, 034008 (1999), arXiv:hep-ph/9901281.
- [57] J. Jalilian-Marian, A. Kovner, A. Leonidov, and H. Weigert, *Nucl. Phys. B* **504**, 415 (1997), arXiv:hep-ph/9701284.
- [58] J. Jalilian-Marian, A. Kovner, A. Leonidov, and H. Weigert, *Phys. Rev. D* **59**, 014014 (1998), arXiv:hep-ph/9706377 [hep-ph].
- [59] A. Kovner, J. G. Milhano, and H. Weigert, *Phys. Rev. D* **62**, 114005 (2000), arXiv:hep-ph/0004014.
- [60] H. Weigert, *Nucl. Phys. A* **703**, 823 (2002), arXiv:hep-ph/0004044.
- [61] E. Iancu, A. Leonidov, and L. D. McLerran, *Nucl. Phys. A* **692**, 583 (2001), arXiv:hep-ph/0011241.
- [62] E. Iancu, A. Leonidov, and L. D. McLerran, *Phys. Lett. B* **510**, 133 (2001), arXiv:hep-ph/0102009.
- [63] E. Ferreira, E. Iancu, A. Leonidov, and L. McLerran, *Nucl. Phys. A* **703**, 489 (2002), arXiv:hep-ph/0109115.
- [64] E. Kuraev, L. Lipatov, and V. S. Fadin, *Sov. Phys. JETP* **45**, 199 (1977).
- [65] I. Balitsky and L. Lipatov, *Sov. J. Nucl. Phys.* **28**, 822 (1978).
- [66] E. Iancu, A. H. Mueller, D. N. Triantafyllopoulos, and S. Y. Wei, *JHEP* **07**, 196 (2021), arXiv:2012.08562 [hep-ph].
- [67] T. Altinoluk and R. Boussarie, *JHEP* **10**, 208 (2019), arXiv:1902.07930 [hep-ph].
- [68] B. Badelek, J. Kwiecinski, and A. Stasto, *Z. Phys. C* **74**, 297 (1997), arXiv:hep-ph/9603230.
- [69] B. Badelek and A. M. Staśto, *Phys. Lett. B* **829**, 137086 (2022), arXiv:2202.04223 [hep-ph].
- [70] C. G. Callan, Jr. and D. J. Gross, *Phys. Rev. Lett.* **22**, 156 (1969).
- [71] R. K. Ellis, W. J. Stirling, and B. R. Webber, *QCD and collider physics*, Vol. 8 (Cambridge University Press, 2011).
- [72] J. Bartels, K. J. Golec-Biernat, and K. Peters, *Eur. Phys. J. C* **17**, 121 (2000), arXiv:hep-ph/0003042.
- [73] K. Golec-Biernat and A. M. Stasto, *Phys. Rev. D* **80**, 014006 (2009), arXiv:0905.1321 [hep-ph].
- [74] G. R. Boroun, *Eur. Phys. J. A* **43**, 335 (2010), arXiv:1402.1186 [hep-ph].
- [75] G. R. Boroun and B. Rezaei, *Phys. Lett. B* **816**, 136274 (2021), arXiv:2010.15357 [hep-ph].
- [76] See Supplemental Material, which includes Ref. [114–127], for more details on the derivation of Eq. (17).
- [77] R. Baier, Y. L. Dokshitzer, A. H. Mueller, S. Peigne, and D. Schiff, *Nucl. Phys. B* **484**, 265 (1997), arXiv:hep-ph/9608322.
- [78] F. Dominguez, B.-W. Xiao, and F. Yuan, *Phys. Rev. Lett.* **106**, 022301 (2011), arXiv:1009.2141 [hep-ph].
- [79] P. Caucal, F. Salazar, and R. Venugopalan, *JHEP* **11**, 222 (2021), arXiv:2108.06347 [hep-ph].
- [80] P. Caucal, E. Ferrand, and F. Salazar, *JHEP* **05**, 110 (2024), arXiv:2401.01934 [hep-ph].
- [81] A. Ayala, M. Hentschinski, J. Jalilian-Marian, and M. E. Tejeda-Yeomans, *Phys. Lett. B* **761**, 229 (2016), arXiv:1604.08526 [hep-ph].
- [82] A. Ayala, M. Hentschinski, J. Jalilian-Marian, and M. E. Tejeda-Yeomans, *Nucl. Phys. B* **920**, 232 (2017), arXiv:1701.07143 [hep-ph].
- [83] F. Bergabo and J. Jalilian-Marian, *JHEP* **01**, 095 (2023), arXiv:2210.03208 [hep-ph].
- [84] For general kinematics, this divergence is cancelled by the high energy evolution of the dipole S -matrix [80].
- [85] M. Boglione, J. Collins, L. Gamberg, J. O. Gonzalez-Hernandez, T. C. Rogers, and N. Sato, *Phys. Lett. B* **766**, 245 (2017), arXiv:1611.10329 [hep-ph].
- [86] X.-B. Tong, B.-W. Xiao, and Y.-Y. Zhang, *Phys. Rev. Lett.* **130**, 151902 (2023), arXiv:2211.01647 [hep-ph].
- [87] E. Iancu, A. H. Mueller, and D. N. Triantafyllopoulos, *Phys. Rev. Lett.* **128**, 202001 (2022), arXiv:2112.06353 [hep-ph].
- [88] Y. Hatta, B.-W. Xiao, and F. Yuan, *Phys. Rev. D* **106**, 094015 (2022), arXiv:2205.08060 [hep-ph].
- [89] S. Hauksson, E. Iancu, A. H. Mueller, D. N. Triantafyllopoulos, and S. Y. Wei, *JHEP* **06**, 180 (2024), arXiv:2402.14748 [hep-ph].
- [90] P. Caucal and E. Iancu, (2024), arXiv:2406.04238 [hep-ph].
- [91] M. Hentschinski, A. Kusina, K. Kutak, and M. Serino, *Eur. Phys. J. C* **78**, 174 (2018), arXiv:1711.04587 [hep-ph].
- [92] G. Altarelli and G. Martinelli, *Phys. Lett. B* **76**, 89 (1978).
- [93] M. Gluck and E. Reya, *Nucl. Phys. B* **145**, 24 (1978).
- [94] K.-B. Chen, J.-P. Ma, and X.-B. Tong, *JHEP* **05**, 298 (2024), arXiv:2402.15112 [hep-ph].
- [95] M. A. Ebert, J. K. L. Michel, I. W. Stewart, and Z. Sun, *JHEP* **07**, 129 (2022), arXiv:2201.07237 [hep-ph].
- [96] O. del Rio, A. Prokudin, I. Scimemi, and A. Vladimirov, *Phys. Rev. D* **110**, 016003 (2024), arXiv:2402.01836 [hep-ph].
- [97] L. D. McLerran and R. Venugopalan, *Phys. Rev. D* **49**, 3352 (1994), arXiv:hep-ph/9311205.
- [98] L. D. McLerran and R. Venugopalan, *Phys. Rev. D* **49**, 2233 (1994), arXiv:hep-ph/9309289.
- [99] T. Lappi and H. Mäntysaari, *Phys. Rev. D* **88**, 114020 (2013), arXiv:1309.6963 [hep-ph].
- [100] V. Cheung, Z.-B. Kang, F. Salazar, and R. Vogt, *Phys. Rev. D* **110**, 094039 (2024), arXiv:2409.04080 [hep-ph].
- [101] B. G. Giraud and R. Peschanski, *Phys. Lett. B* **760**, 26 (2016), arXiv:1604.01932 [hep-ph].
- [102] B. Ducloué, E. Iancu, G. Soyez, and D. Triantafyllopoulos, *Phys. Lett. B* **803**, 135305 (2020), arXiv:1912.09196 [hep-ph].
- [103] V. V. Sudakov, *Sov. Phys. JETP* **3**, 65 (1956).
- [104] Y. L. Dokshitzer, D. Diakonov, and S. I. Troian, *Phys. Rept.* **58**, 269 (1980).
- [105] G. Parisi and R. Petronzio, *Nucl. Phys. B* **154**, 427 (1979).
- [106] J. C. Collins, D. E. Soper, and G. F. Sterman, *Nucl. Phys. B* **250**, 199 (1985).
- [107] A. H. Mueller, B.-W. Xiao, and F. Yuan, *Phys. Rev. Lett.* **110**, 082301 (2013), arXiv:1210.5792 [hep-ph].
- [108] A. Mueller, B.-W. Xiao, and F. Yuan, *Phys. Rev. D* **88**, 114010 (2013), arXiv:1308.2993 [hep-ph].
- [109] P. Caucal, F. Salazar, B. Schenke, and R. Venugopalan, *JHEP* **11**, 169 (2022), arXiv:2208.13872 [hep-ph].
- [110] P. Tael, T. Altinoluk, G. Beuf, and C. Marquet, *JHEP* **10**, 184 (2022), arXiv:2204.11650 [hep-ph].

- [111] T. Altinoluk, J. Jalilian-Marian, and C. Marquet, *Phys. Rev. D* **110**, 094056 (2024), arXiv:2406.08277 [hep-ph].
- [112] P. Caucal, F. Salazar, B. Schenke, T. Stebel, and R. Venugopalan, *Phys. Rev. Lett.* **132**, 081902 (2024), arXiv:2308.00022 [hep-ph].
- [113] D. Binosi and L. Theussl, *Comput.Phys.Commun.* **161**, 76 (2004), arXiv:hep-ph/0309015 [hep-ph].
- [114] K. Roy and R. Venugopalan, *Phys. Rev. D* **101**, 034028 (2020), arXiv:1911.04530 [hep-ph].
- [115] E. C. Aschenauer, S. Fazio, M. A. C. Lamont, H. Paukkunen, and P. Zurita, *Phys. Rev. D* **96**, 114005 (2017), arXiv:1708.05654 [nucl-ex].
- [116] H. Kowalski and D. Teaney, *Phys.Rev.* **D68**, 114005 (2003), arXiv:hep-ph/0304189 [hep-ph].
- [117] A. H. Rezaeian, M. Siddikov, M. Van de Klundert, and R. Venugopalan, *Phys.Rev.* **D87**, 034002 (2013), arXiv:1212.2974.
- [118] N. Armesto, T. Lappi, H. Mäntysaari, H. Paukkunen, and M. Tevio, *Phys. Rev. D* **105**, 114017 (2022), arXiv:2203.05846 [hep-ph].
- [119] L. P. Kaptari, A. V. Kotikov, N. Y. Chernikova, and P. Zhang, *Phys. Rev. D* **99**, 096019 (2019), arXiv:1904.04405 [hep-ph].
- [120] T. Altinoluk, G. Beuf, A. Czajka, and A. Tymowska, *Phys. Rev. D* **104**, 014019 (2021), arXiv:2012.03886 [hep-ph].
- [121] T. Altinoluk and G. Beuf, *Phys. Rev. D* **105**, 074026 (2022), arXiv:2109.01620 [hep-ph].
- [122] T. Altinoluk, G. Beuf, A. Czajka, and A. Tymowska, *Phys. Rev. D* **107**, 074016 (2023), arXiv:2212.10484 [hep-ph].
- [123] R. Boussarie and Y. Mehtar-Tani, *Phys. Lett. B* **831**, 137125 (2022), arXiv:2006.14569 [hep-ph].
- [124] R. Boussarie and Y. Mehtar-Tani, *JHEP* **07**, 080 (2022), arXiv:2112.01412 [hep-ph].
- [125] R. Boussarie and Y. Mehtar-Tani, *JHEP* **10**, 056 (2024), arXiv:2309.16576 [hep-ph].
- [126] Y. Fu, Z.-B. Kang, F. Salazar, X.-N. Wang, and H. Xing, (2023), arXiv:2310.12847 [hep-ph].
- [127] Y. Fu, Z.-B. Kang, F. Salazar, X.-N. Wang, and H. Xing, (2024), arXiv:2406.01684 [hep-ph].

Supplemental Material

A. Leading twist contribution to F_L from the LO structure function $F_{UU,L}^{\text{LO}}$ for semi-inclusive DIS jet production

In this Supplemental Material, we demonstrate that although $F_{UU,L}^{\text{LO}}$ given by Eq. (3) in the main text is power suppressed by P_\perp^2/Q^2 , the integral over \mathbf{P}_\perp of Eq. (3) provides at leading power contribution to F_L proportional to the gluon PDF. For phenomenological studies of the longitudinal structure function at small x , we refer the reader to [74, 75, 115–119].

By definition, at this leading perturbative order where jets and partons are in one-to-one correspondence,

$$F_L(x, Q^2) \equiv \int d^2\mathbf{P}_\perp F_{UU,L}^{\text{LO}}(x, Q^2, \mathbf{P}_\perp). \quad (21)$$

The integral over \mathbf{P}_\perp can be performed analytically, such that

$$F_L(x, Q^2) = \frac{N_c}{\pi^3} \int_{\mathbf{B}_\perp, \mathbf{q}_\perp} \mathcal{D}_F(x, \mathbf{q}_\perp) \int_0^1 dz \bar{Q}^2 \left[1 - \frac{2\bar{Q}^2}{q_\perp^2 \sqrt{1 + 4\bar{Q}^2/q_\perp^2}} \ln \left(1 + \frac{q_\perp^2}{2\bar{Q}^2} \left[1 + \sqrt{1 + 4\bar{Q}^2/q_\perp^2} \right] \right) \right]. \quad (22)$$

Expanding the quantity inside the z integral for $Q^2 \gg q_\perp^2 \sim Q_s^2$, we get

$$\bar{Q}^2 \left[1 - \frac{2\bar{Q}^2}{q_\perp^2 \sqrt{1 + 4\bar{Q}^2/q_\perp^2}} \ln \left(1 + \frac{q_\perp^2 \left[1 + \sqrt{1 + 4\bar{Q}^2/q_\perp^2} \right]}{2\bar{Q}^2} \right) \right] = \frac{q_\perp^2}{6} + \mathcal{O} \left(\frac{q_\perp^4}{\bar{Q}^2} \right), \quad (23)$$

which is independent of z at the lowest order in the $1/Q$ expansion. This means that the z integral is not controlled by the end-points $z = 0$ and $z = 1$. Performing the trivial integration over z , we get

$$F_L(x, Q^2) = \frac{N_c}{6\pi^3} \int_{\mathbf{B}_\perp} \int^{Q^2} d^2\mathbf{q}_\perp q_\perp^2 \mathcal{D}_F(x, \mathbf{q}_\perp), \quad (24)$$

where the logarithmically divergent \mathbf{q}_\perp integral is cut by the large virtuality scale $q_\perp^2 \leq Q^2$ in agreement with our $Q^2 \gg q_\perp^2$ initial assumption. Using the definition of the gluon PDF at small x given by Eq. (6) in the main text, one finds the gluon contribution to F_L ,

$$F_L^g(x, Q^2) = \frac{\alpha_s}{3\pi} xg(x, Q^2), \quad \text{for } x \ll 1. \quad (25)$$

This is in agreement with the Altarelli-Martinelli formula for F_L [92, 93]:

$$F_L(x, Q^2) = \frac{\alpha_s}{2\pi} x^2 \int_x^1 \frac{dz}{z^3} \left[\frac{8}{3} F_2(z, Q^2) + 4 \left(1 - \frac{x}{z}\right) z g(z, Q^2) \right], \quad (26)$$

with F_2 the standard second DIS structure function. Focusing on the second term alone, approximating $z g(z, Q^2) \approx x g(x, Q^2)$ at small x , and performing the z integral

$$\int_x^1 \frac{dz}{z^3} \left(1 - \frac{x}{z}\right) = \frac{1}{6x^2} [1 + \mathcal{O}(x^2)], \quad (27)$$

we find indeed Eq. (25).

The sea quark contribution to F_L . Formally, Eq. (26) is valid at $\mathcal{O}(\alpha_s)$ and therefore does not contain the contribution from sea quarks. However, one can guess what the connection should be between F_L and the sea quark PDF at small x by using the identity $F_2(x, Q^2) = x q(x, Q^2)$ from the naive parton model (with $x q(x, Q^2)$ the valence quark PDF) and by extending it to the case of sea quarks. For sea quarks at small x , one can approximate $z q(z, Q^2)$ in the z -integral in Eq. (26) by $x q_{\text{sea}}(x, Q^2)$ since $x q_{\text{sea}}(x, Q^2)$ grows like a power law as x decreases. Using

$$x^2 \int_x^1 \frac{dz}{z^3} = \frac{1}{2} + \mathcal{O}(x^2), \quad (28)$$

we get

$$F_L^q(x, Q^2) = \frac{2\alpha_s}{3\pi} x q_{\text{sea}}(x, Q^2) = \frac{\alpha_s C_F}{2\pi} x q_{\text{sea}}(x, Q^2), \quad \text{for } x \ll 1, \quad (29)$$

which is akin to the relation between the LP $F_{UU,L}$ and the sea quark TMD obtained in the main text.

B. Proof of Eq. (11) in the main text

In this Supplemental Material, we provide the mathematical proof of Eq. (11) in the Letter. Our starting point is Eq. (7) in the Letter. After making the approximations discussed in the main text and the change of transverse coordinate variables $\mathbf{x}_\perp, \mathbf{y}_\perp, \mathbf{x}'_\perp, \mathbf{z}_\perp \rightarrow \mathbf{B}_\perp = (\mathbf{x}_\perp + \mathbf{x}'_\perp)/2, \mathbf{r}_{xy} = \mathbf{x}_\perp - \mathbf{y}_\perp, \mathbf{r}_{x'y} = \mathbf{x}'_\perp - \mathbf{y}_\perp, \mathbf{r}_{zy} = \mathbf{z}_\perp - \mathbf{y}_\perp$, Eq. (7) becomes

$$F_{UU,L}^{\text{R1} \times \text{R1}^*} = \frac{\alpha_s N_c}{16\pi^8} \int d^2 \mathbf{q}_\perp \int_{\mathbf{B}_\perp, \mathbf{r}_{xy}, \mathbf{r}_{x'y}, \mathbf{r}_{zy}} e^{-i\mathbf{P}_\perp \cdot (\mathbf{r}_{xy} - \mathbf{r}_{x'y})} \int_0^1 dz \int_0^1 dz_g z_g (1 - z_g)^2 Q^4 K_0(Q X_R) K_0(Q X'_R) \\ \times \frac{\mathbf{r}_{xy} \cdot \mathbf{r}_{x'y}}{\mathbf{r}_{xy}^2 \mathbf{r}_{x'y}^2} (e^{i\mathbf{q}_\perp \cdot \mathbf{r}_{xy}} - 1) (e^{-i\mathbf{q}_\perp \cdot \mathbf{r}_{x'y}} - 1) C_F \mathcal{D}_F(x, \mathbf{q}_\perp), \quad (30)$$

with $X_R = z \mathbf{r}_{xy} + z_g (1 - z_g) \mathbf{r}_{zy}$ and $X'_R = z \mathbf{r}_{x'y} + z_g (1 - z_g) \mathbf{r}_{zy}$. The first trick is to introduce the unity in Eq. (30) with

$$1 = \int \frac{d^2 \mathbf{l}_{3\perp}}{(2\pi)^2} \int d^2 \mathbf{r}_{z'y} e^{i\mathbf{l}_{3\perp} \cdot (\mathbf{r}_{zy} - \mathbf{r}_{z'y})} = \int d^2 \mathbf{r}_{z'y} \delta^{(2)}(\mathbf{r}_{zy} - \mathbf{r}_{z'y}), \quad (31)$$

which allows us to replace \mathbf{r}_{zy} by $\mathbf{r}_{z'y}$ in X'_R . Since we work under the assumption $r_{zy} \sim 1/Q$, it means that the auxiliary momentum scale $|\mathbf{l}_{3\perp}|$ is also of order Q . Grouping together the integrals over transverse coordinates with and without prime indices, we get

$$F_{UU,L}^{\text{R1} \times \text{R1}^*} = \frac{\alpha_s C_F N_c}{2\pi^5} Q^2 \int_0^1 dz \int_0^1 dz_g z_g (1 - z_g)^2 \int_{\mathbf{B}_\perp, \mathbf{q}_\perp} \mathcal{D}_F(x, \mathbf{q}_\perp) \int \frac{d^2 \mathbf{l}_{3\perp}}{(2\pi)^2} \mathcal{H}_{\text{R1} \times \text{R1}^*}^i \mathcal{H}_{\text{R1} \times \text{R1}^*}^{i*}, \quad (32)$$

with the ‘‘hard factor’’ of diagram $\text{R1} \times \text{R1}^*$ defined as

$$\mathcal{H}_{\text{R1} \times \text{R1}^*}^i \equiv \int \frac{d^2 \mathbf{r}_{xy}}{(2\pi)^2} \int \frac{d^2 \mathbf{r}_{zy}}{(2\pi)^2} e^{-i\mathbf{P}_\perp \cdot \mathbf{r}_{xy}} (e^{i\mathbf{q}_\perp \cdot \mathbf{r}_{xy}} - 1) e^{i\mathbf{l}_{3\perp} \cdot \mathbf{r}_{zy}} \frac{Q \mathbf{r}_{xy}^i}{\mathbf{r}_{xy}^2} K_0 \left(\Delta \sqrt{\mathbf{r}_{zy}^2 + \omega \mathbf{r}_{xy}^2} \right), \quad (33)$$

where $\Delta^2 = z_g(1 - z_g)Q^2$ and $\omega = z/(z_g(1 - z_g))$. The hard factor $\mathcal{H}_{R1 \times R1^*}$ can be computed analytically by using the inverse Fourier transform of the K_0 modified Bessel function (see e.g. [79, 114]):

$$\frac{r_{xy}^i}{r_{xy}^2} K_0 \left(\Delta \sqrt{r_{zy}^2 + \omega r_{xy}^2} \right) = -i \int \frac{d^2 \mathbf{l}_{1\perp}}{(2\pi)} \int \frac{d^2 \mathbf{l}_{2\perp}}{(2\pi)} \frac{\mathbf{l}_{2\perp}^k e^{i \mathbf{l}_{1\perp} \cdot \mathbf{r}_{zy} + i \mathbf{l}_{2\perp} \cdot \mathbf{r}_{xy}}}{(\mathbf{l}_{1\perp}^2 + \Delta^2) [\mathbf{l}_{2\perp}^2 + \omega (\mathbf{l}_{1\perp}^2 + \Delta^2)]}, \quad (34)$$

such that

$$\mathcal{H}_{R1 \times R1^*}^i = \frac{-i(\mathbf{P}_\perp^i - \mathbf{q}_\perp^i)Q}{(\mathbf{l}_{3\perp}^2 + \Delta^2)[(\mathbf{P}_\perp - \mathbf{q}_\perp)^2 + \omega(\mathbf{l}_{3\perp}^2 + \Delta^2)]} + \frac{i\mathbf{P}_\perp^i Q}{(\mathbf{l}_{3\perp}^2 + \Delta^2)[P_\perp^2 + \omega(\mathbf{l}_{3\perp}^2 + \Delta^2)]}. \quad (35)$$

We observe that one is not allowed to make any further approximation in this hard factor, since $|\mathbf{l}_{3\perp}| \sim Q \sim \Delta$ and $P_\perp^2 \sim \omega \mathbf{l}_{3\perp}^2 \sim zQ^2$. Fortunately, we can perform the auxiliary $\mathbf{l}_{3\perp}$ integral analytically, such that

$$\begin{aligned} \int \frac{d^2 \mathbf{l}_{3\perp}}{(2\pi)} \mathcal{H}_{R1 \times R1^*}^i \mathcal{H}_{R1 \times R1^*}^{i*} &= \frac{\bar{Q}^2}{2z_g(1 - z_g)} \left[\frac{1}{P_\perp^2 \bar{Q}^2} + \frac{1}{P_\perp^2 (P_\perp^2 + \bar{Q}^2)} - \frac{2 \ln(1 + P_\perp^2 / \bar{Q}^2)}{P_\perp^4} + \frac{1}{(\mathbf{P}_\perp - \mathbf{q}_\perp)^2 \bar{Q}^2} \right. \\ &+ \frac{1}{(\mathbf{P}_\perp - \mathbf{q}_\perp)^2 ((\mathbf{P}_\perp - \mathbf{q}_\perp)^2 + \bar{Q}^2)} - \frac{2 \ln(1 + (\mathbf{P}_\perp - \mathbf{q}_\perp)^2 / \bar{Q}^2)}{(\mathbf{P}_\perp - \mathbf{q}_\perp)^4} - 2 \frac{\mathbf{P}_\perp \cdot (\mathbf{P}_\perp - \mathbf{q}_\perp)}{P_\perp^4 (\mathbf{P}_\perp - \mathbf{q}_\perp)^4 (P_\perp^2 - (\mathbf{P}_\perp - \mathbf{q}_\perp)^2)} \\ &\left. \times \left(\frac{(P_\perp^2 - (\mathbf{P}_\perp - \mathbf{q}_\perp)^2)(\mathbf{P}_\perp - \mathbf{q}_\perp)^2 P_\perp^2}{\bar{Q}^2} + (\mathbf{P}_\perp - \mathbf{q}_\perp)^4 \ln(1 + P_\perp^2 / \bar{Q}^2) - P_\perp^4 \ln(1 + (\mathbf{P}_\perp - \mathbf{q}_\perp)^2 / \bar{Q}^2) \right) \right], \quad (36) \end{aligned}$$

with $\bar{Q}^2 = zQ^2$. The integral over z_g in Eq. (32) becomes trivial since z_g does not appear inside the square bracket of Eq. (36):

$$\int_0^1 dz_g (1 - z_g) = \frac{1}{2}. \quad (37)$$

The last step is to do the z integral and to take the limit $Q \gg P_\perp$ of the result. These two manipulations can be performed together thanks to the change of variable $z \rightarrow u = zQ^2/P_\perp^2$, such that the integral over u goes from 0 to $Q^2/P_\perp^2 \rightarrow \infty$ in the limit $Q^2 \gg P_\perp^2$:

$$\begin{aligned} F_{UU,L}^{R1 \times R1^*} &= \frac{\alpha_s C_F N_c}{8\pi^5} \int_{\mathbf{B}_\perp, \mathbf{q}_\perp} \mathcal{D}_F(x, \mathbf{q}_\perp) \int_0^\infty du \, 2u \left[\frac{1}{u} + \frac{1}{1+u} - 2 \ln \left(1 + \frac{1}{u} \right) - \frac{\mathbf{P}_\perp \cdot (\mathbf{P}_\perp - \mathbf{q}_\perp)}{(P_\perp^2 - (\mathbf{P}_\perp - \mathbf{q}_\perp)^2)} \right. \\ &\left. \times \left(\frac{P_\perp^2 - (\mathbf{P}_\perp - \mathbf{q}_\perp)^2}{(\mathbf{P}_\perp - \mathbf{q}_\perp)^2 u} + \ln \left(1 + \frac{1}{u} \right) - \frac{P_\perp^4}{(\mathbf{P}_\perp - \mathbf{q}_\perp)^4} \ln \left(1 + \frac{(\mathbf{P}_\perp - \mathbf{q}_\perp)^2}{P_\perp^2 u} \right) \right) \right] \quad (38) \end{aligned}$$

$$= \frac{\alpha_s C_F}{2\pi} \times \frac{N_c}{4\pi^4} \int_{\mathbf{B}_\perp, \mathbf{q}_\perp} \mathcal{D}_F(x, \mathbf{q}_\perp) \left[1 - \frac{\mathbf{P}_\perp \cdot (\mathbf{P}_\perp - \mathbf{q}_\perp) \ln(P_\perp^2 / (\mathbf{P}_\perp - \mathbf{q}_\perp)^2)}{(P_\perp^2 - (\mathbf{P}_\perp - \mathbf{q}_\perp)^2)} \right], \quad (39)$$

which is exactly the result given by Eq. (11) in the main text. The integral over u is controlled by $u \lesssim 1$, meaning that the z integration is dominated by the physical endpoint $z \sim P_\perp^2/Q^2$ as discussed in the main text. It is remarkable that the integral over u coming from the complicated momentum space hard factor in Eq. (36) eventually gives the same P_\perp dependence as for the sea quark TMD involved in the transversely polarised photon case at LO.

C. Proof of Eqs. (14)-(15) in the main text

We now turn to the derivation of the leading power contribution coming from a gluon jet measurement in single-inclusive jet production in DIS mediated by a longitudinally polarised virtual photon. The extraction of the LP component out of the coordinate space expressions obtained in [80] is more complicated than in the quark jet case. To cross-check our final result presented in the last subsection and given by Eq. (15) in the main text, we have performed an independent calculation based on the momentum space expression of the cross-section for $\gamma_L^* + A \rightarrow q\bar{q}$ +gluon with $z_g \sim P_\perp^2/Q^2 \ll 1$ production, in which the $q\bar{q}$ pair is subsequently integrated out.

In the following, we divide the calculation into three contributions according to the notations of [80]:

- (i) the NLO-4 term coming from Feynman graphs where the gluon is emitted before the shockwave both in the amplitude and in the complex conjugate amplitude (cf. bottom-left diagram in Fig. (1) of the Letter),
- (ii) the NLO-1 term coming from interferences between gluon emission before and after the shockwave and,
- (iii) the NLO-0+NLO-3 terms coming from diagrams where the gluon is emitted after the shockwave both in the amplitude and complex conjugate amplitude (cf. bottom-right diagram in Fig. (1) of the Letter).

The NLO-4 contribution

The contribution of Eq. (3.73) in [80] to $F_{UU,L}$ reads

$$F_{UU,L}^{\text{NLO4}} = \frac{\alpha_s N_c}{4\pi^8} \int_{\mathbf{x}_\perp, \mathbf{y}_\perp, \mathbf{z}_\perp, \mathbf{z}'_\perp} e^{-i\mathbf{P}_\perp \cdot \mathbf{r}_{zz'}} \int_0^1 \frac{dz}{z} \int_0^{1-z} dz_1 z_1^2 (1-z_1-z)^2 Q^4 K_0(QX_R) K_0(QX'_R) \\ \times \Re \left[\Xi_{\text{NLO4,g}}(\mathbf{x}_\perp, \mathbf{y}_\perp, \mathbf{z}_\perp, \mathbf{z}'_\perp) \left[\left(1 + \frac{z}{z_1} + \frac{z^2}{2z_1^2} \right) \frac{\mathbf{r}_{zx} \cdot \mathbf{r}_{z'x}}{\mathbf{r}_{zx}^2 \mathbf{r}_{z'x}^2} - \left(1 + \frac{z}{2z_1} + \frac{z}{2(1-z_1-z)} \right) \frac{\mathbf{r}_{zy} \cdot \mathbf{r}_{z'x}}{\mathbf{r}_{zy}^2 \mathbf{r}_{z'x}^2} \right] \right], \quad (40)$$

with the CGC correlator given by

$$\Xi_{\text{NLO4,g}}(\mathbf{x}_\perp, \mathbf{y}_\perp, \mathbf{z}_\perp, \mathbf{z}'_\perp) = \frac{N_c}{2} \langle 1 - D_{xz} D_{zy} - D_{yz'} D_{z'x} + D_{z'z} D_{zz'} \rangle_x - \frac{1}{2N_c} \langle 2 - D_{xy} - D_{yx} \rangle, \quad (41)$$

and the effective size of the $q\bar{q}g$ system

$$X_R = z_1(1-z_1-z)\mathbf{r}_{xy}^2 + z_1 z \mathbf{r}_{zx}^2 + (1-z_1-z)z \mathbf{r}_{zy}^2, \quad (42)$$

$$X'_R = z_1(1-z_1-z)\mathbf{r}_{xy}^2 + z_1 z \mathbf{r}_{z'x}^2 + (1-z_1-z)z \mathbf{r}_{z'y}^2. \quad (43)$$

Note that since the gluon-jet is tagged, we have $z_g = z$ and we integrate over the longitudinal momentum fraction z_1 of the quark.

We first do a change of transverse coordinates using $\mathbf{B}_\perp = z_1 \mathbf{x}_\perp + (1-z_1) \mathbf{y}_\perp$ and $\mathbf{r}_{xy} = \mathbf{x}_\perp - \mathbf{y}_\perp$. Note that since $z \ll 1$, \mathbf{B}_\perp physically corresponds to the impact parameter of the virtual photon. We then implement the approximations discussed in the main text, namely (i) the integral over z is dominated by $z \sim P_\perp^2/Q^2 \ll 1$ when $Q^2 \gg P_\perp^2$, (ii) the integral over transverse coordinates is controlled by dipole sizes such that $r_{xy} \sim 1/Q$ and $r_{zB} \sim r_{z'B} \sim 1/P_\perp$.

In this limit, we have $X_R \approx z_1(1-z_1)\mathbf{r}_{xy}^2 + z\mathbf{r}_{zB}^2$ and $X'_R \approx z_1(1-z_1)\mathbf{r}_{xy}^2 + z\mathbf{r}_{z'B}^2$. The next step is to expand $\Xi_{\text{NLO4,g}}$ in the regime $r_{xy} \ll r_{zB}, r_{z'B}$:

$$\Re(\Xi_{\text{NLO4,g}}(\mathbf{x}_\perp, \mathbf{y}_\perp, \mathbf{z}_\perp, \mathbf{z}'_\perp)) = \frac{N_c}{2} \Re \langle 1 - D_{Bz} D_{zB} - D_{Bz'} D_{z'B} + D_{zz'} D_{z'z} \rangle \\ - (1-2z_1) \mathbf{r}_{xy}^i \frac{N_c}{2} \Re \left\langle \frac{1}{N_c^2} \text{Tr}(V_B V_z^\dagger) \text{Tr}(V_z \partial^i V_B^\dagger) \right\rangle - (1-2z_1) \mathbf{r}_{xy}^i \frac{N_c}{2} \Re \left\langle \frac{1}{N_c^2} \text{Tr}(\partial^i V_B V_{z'}^\dagger) \text{Tr}(V_{z'} V_B^\dagger) \right\rangle + \mathcal{O}(r_{xy}^2), \quad (44)$$

where the terms of order r_{xy}^2 can be neglected as they would necessarily yield $1/Q^2$ suppressed contributions after forming the product with the quantity inside the square bracket in Eq. (40).

Indeed, this quantity must be similarly expanded up to the order $\mathcal{O}(r_{xy}^2)$ or $\mathcal{O}(z)$, as

$$\left[\left(1 + \frac{z}{z_1} + \frac{z^2}{2z_1^2} \right) \frac{\mathbf{r}_{zx} \cdot \mathbf{r}_{z'x}}{\mathbf{r}_{zx}^2 \mathbf{r}_{z'x}^2} - \left(1 + \frac{z}{2z_1} + \frac{z}{2(1-z_1-z)} \right) \frac{\mathbf{r}_{zy} \cdot \mathbf{r}_{z'x}}{\mathbf{r}_{zy}^2 \mathbf{r}_{z'x}^2} \right] \approx - \frac{\mathbf{r}_{z'B}^i \mathbf{r}_{xy}^j}{\mathbf{r}_{z'B}^2 \mathbf{r}_{zB}^2} \left[\delta^{ij} - \frac{2\mathbf{r}_{zB}^i \mathbf{r}_{zB}^j}{\mathbf{r}_{zB}^2} \right] \\ + \frac{z(1-2z_1)}{2z_1(1-z_1)} \frac{\mathbf{r}_{zB} \cdot \mathbf{r}_{z'B}}{\mathbf{r}_{zB}^2 \mathbf{r}_{z'B}^2} + (1-z_1) \frac{\mathbf{r}_{xy}^j \mathbf{r}_{xy}^k}{\mathbf{r}_{zB}^2 \mathbf{r}_{z'B}^2} \left[\delta^{ij} - \frac{2\mathbf{r}_{zB}^i \mathbf{r}_{zB}^j}{\mathbf{r}_{zB}^2} \right] \left[\delta^{ik} - \frac{2\mathbf{r}_{z'B}^i \mathbf{r}_{z'B}^k}{\mathbf{r}_{z'B}^2} \right] + \mathcal{O}(z^2, r_{xy}^3). \quad (45)$$

In order to get a leading power contribution, one should consider the terms in the product between Eq. (44) and Eq. (45) which are at most $\mathcal{O}(z^0 r_{xy}^2)$ or $\mathcal{O}(z^1 r_{xy}^0)$. Among those terms, the only one which is not proportional to $1-2z_1$ is

$$\frac{N_c}{2} \Re \langle 1 - D_{Bz} D_{zB} - D_{Bz'} D_{z'B} + D_{zz'} D_{z'z} \rangle \times (1-z_1) \frac{\mathbf{r}_{xy}^j \mathbf{r}_{xy}^k}{\mathbf{r}_{zB}^2 \mathbf{r}_{z'B}^2} \left[\delta^{ij} - \frac{2\mathbf{r}_{zB}^i \mathbf{r}_{zB}^j}{\mathbf{r}_{zB}^2} \right] \left[\delta^{ik} - \frac{2\mathbf{r}_{z'B}^i \mathbf{r}_{z'B}^k}{\mathbf{r}_{z'B}^2} \right]. \quad (46)$$

It is easy to check that the terms proportional to $1-2z_1$ will cancel after integrating over z_1 , since

$$\int_0^1 dz_1 (1-2z_1) = 0. \quad (47)$$

The CGC correlator in Eq. (46) can be fully written in term of the gluon-gluon dipole $D_{xz'}^g$,

$$D_{Bz}^g \equiv \frac{1}{N_c^2 - 1} U_{\mathbf{B}_\perp}^{ab} U_{\mathbf{z}_\perp}^{\dagger,ba}, \quad (48)$$

by mean of the Fierz identity, such that

$$D_{Bz} D_{zB} = \frac{N_c^2 - 1}{N_c^2} D_{Bz}^g + \frac{1}{N_c^2}. \quad (49)$$

Using this equation, we find that the CGC correlator in Eq. (46) reduces to a sum of gluon-gluon dipoles as discussed in the main text:

$$\frac{N_c}{2} \Re \langle 1 - D_{Bz} D_{zB} - D_{Bz'} D_{z'B} + D_{zz'} D_{z'z} \rangle = C_F \langle 1 - D_{zB}^g - D_{Bz'}^g + D_{z'z'}^g \rangle_x, \quad (50)$$

$$= C_F \int_{\mathbf{q}_\perp} (e^{i\mathbf{q}_\perp \cdot \mathbf{r}_{zB}} - 1) (e^{-i\mathbf{q}_\perp \cdot \mathbf{r}_{z'B}} - 1) \mathcal{D}_A(x, \mathbf{q}_\perp). \quad (51)$$

Combining all these results together, the leading power contribution of Eq. (40) can be expressed as

$$F_{UU,L}^{\text{NLO4,LP}} = \frac{\alpha_s N_c}{4\pi^8} \int_{\mathbf{B}_\perp, \mathbf{r}_{xy}, \mathbf{r}_{zB}, \mathbf{r}_{z'B}} e^{-i\mathbf{P}_\perp \cdot \mathbf{r}_{zz'}} C_F \Re \int_{\mathbf{q}_\perp} (e^{i\mathbf{q}_\perp \cdot \mathbf{r}_{zB}} - 1) (e^{-i\mathbf{q}_\perp \cdot \mathbf{r}_{z'B}} - 1) \mathcal{D}_A(x, \mathbf{q}_\perp) \\ \times \int_0^1 \frac{dz}{z} \int_0^1 dz_1 z_1^2 (1 - z_1)^3 Q^4 K_0(QX_R) K_0(QX'_R) \frac{\mathbf{r}_{xy}^j \mathbf{r}_{xy}^k}{\mathbf{r}_{zB}^2 \mathbf{r}_{z'B}^2} \left[\delta^{ij} - \frac{2\mathbf{r}_{zB}^i \mathbf{r}_{zB}^j}{\mathbf{r}_{zB}^2} \right] \left[\delta^{ik} - \frac{2\mathbf{r}_{z'B}^i \mathbf{r}_{z'B}^k}{\mathbf{r}_{z'B}^2} \right] \quad (52)$$

$$= \frac{2\alpha_s C_F N_c Q^2}{\pi^5} \int_0^1 \frac{dz}{z} \int_0^1 dz_1 \int_{\mathbf{B}_\perp, \mathbf{q}_\perp} \mathcal{D}_A(x, \mathbf{q}_\perp) z_1 (1 - z_1)^2 \int \frac{d^2 \mathbf{l}_{3\perp}}{(2\pi)} \mathcal{H}_{\text{NLO4}}^i \mathcal{H}_{\text{NLO4}}^{i*}, \quad (53)$$

with

$$\mathcal{H}_{\text{NLO4}}^i = \int \frac{d^2 \mathbf{r}_{zB}}{(2\pi)} \int \frac{d^2 \mathbf{r}_{xy}}{(2\pi)} e^{-i\mathbf{P}_\perp \cdot \mathbf{r}_{zB}} (e^{i\mathbf{q}_\perp \cdot \mathbf{r}_{zB}} - 1) e^{i\mathbf{l}_{3\perp} \cdot \mathbf{r}_{xy}} \frac{\bar{Q}_1 \mathbf{r}_{xy}^k}{\mathbf{r}_{zB}^2} \left[\delta^{ik} - 2 \frac{\mathbf{r}_{zB}^i \mathbf{r}_{zB}^k}{\mathbf{r}_{zB}^2} \right] K_0 \left(\bar{Q}_1 \sqrt{\mathbf{r}_{xy}^2 + \omega \mathbf{r}_{zB}^2} \right), \quad (54) \\ = \frac{-i\bar{Q}_1 (\mathbf{P}_\perp - \mathbf{q}_\perp)^2 \mathbf{l}_{3\perp}^k}{(\mathbf{l}_{3\perp}^2 + \bar{Q}_1^2)^2 ((\mathbf{P}_\perp - \mathbf{q}_\perp)^2 + \omega(\mathbf{l}_{3\perp}^2 + \bar{Q}_1^2))} \left[\delta^{ik} - \frac{2(\mathbf{P}_\perp - \mathbf{q}_\perp)^i (\mathbf{P}_\perp - \mathbf{q}_\perp)^k}{(\mathbf{P}_\perp - \mathbf{q}_\perp)^2} \right] \\ + \frac{i\bar{Q}_1 \mathbf{P}_\perp^2 \mathbf{l}_{3\perp}^k}{(\mathbf{l}_{3\perp}^2 + \bar{Q}_1^2)^2 (\mathbf{P}_\perp^2 + \omega(\mathbf{l}_{3\perp}^2 + \bar{Q}_1^2))} \left[\delta^{ik} - \frac{2\mathbf{P}_\perp^i \mathbf{P}_\perp^k}{\mathbf{P}_\perp^2} \right], \quad (55)$$

where we have introduced the shorthand variables $\bar{Q}_1^2 = z_1(1 - z_1)Q^2$ and $\omega = z/(z_1(1 - z_1))$. To get the second equality, we have used similar tricks as in section B of this Supplemental Material.

Integrating over $\mathbf{l}_{3\perp}$, z_1 and z between some lower cut-off z_0 and 1 yields

$$F_{UU,L}^{\text{NLO4,LP}} = \frac{\alpha_s C_F N_c}{6\pi^5} \int_{\mathbf{B}_\perp, \mathbf{q}_\perp} \mathcal{D}_A(x, \mathbf{q}_\perp) \left[-\frac{11}{6} + \frac{1}{2} \ln \left(\frac{\mathbf{P}_\perp^2}{z_0 Q^2} \right) + \frac{1}{2} \ln \left(\frac{(\mathbf{P}_\perp - \mathbf{q}_\perp)^2}{z_0 Q^2} \right) + \left(1 - \frac{2(\mathbf{P}_\perp \cdot (\mathbf{P}_\perp - \mathbf{q}_\perp))^2}{\mathbf{P}_\perp^2 (\mathbf{P}_\perp - \mathbf{q}_\perp)^2} \right) \right. \\ \left. \times \left(-\frac{5}{6} + \frac{\mathbf{P}_\perp^2 + (\mathbf{P}_\perp - \mathbf{q}_\perp)^2}{2(\mathbf{P}_\perp^2 - (\mathbf{P}_\perp - \mathbf{q}_\perp)^2)} \ln \left(\frac{(\mathbf{P}_\perp - \mathbf{q}_\perp)^2}{\mathbf{P}_\perp^2} \right) + \frac{1}{2} \ln \left(\frac{\mathbf{P}_\perp^2}{z_0 Q^2} \right) + \frac{1}{2} \ln \left(\frac{(\mathbf{P}_\perp - \mathbf{q}_\perp)^2}{z_0 Q^2} \right) \right) \right]. \quad (56)$$

The dependence upon z_0 and Q^2 in this expression will cancel after adding the NLO-1 contribution.

The NLO-1 contribution

Let us now consider the contribution of Eq. (3.72) in [80] to $F_{UU,L}$:

$$F_{UU,L}^{\text{NLO1}} = \frac{\alpha_s N_c}{4\pi^8} \int_{\mathbf{x}_\perp, \mathbf{y}_\perp, \mathbf{z}_\perp, \mathbf{z}'_\perp} e^{-i\mathbf{P}_\perp \cdot \mathbf{r}_{zz'}} \int_0^1 \frac{dz}{z} \int_0^{1-z} dz_1 e^{i\frac{z_1}{z} \mathbf{P}_\perp \cdot \mathbf{r}_{z'x}} z_1^2 (1 - z_1 - z)^2 \left(1 + \frac{z_1}{z} \right) Q^4 K_0(\bar{Q}_{R2} r_{z'y}) K_0(QX_R) \\ \times \Re \left[\Xi_{\text{NLO,1}}(\mathbf{x}_\perp, \mathbf{y}_\perp, \mathbf{z}_\perp, \mathbf{z}'_\perp) \right] \left[\left(1 + \frac{z}{2z_1} + \frac{z}{2(1 - z_1 - z)} \right) \frac{\mathbf{r}_{zy} \cdot \mathbf{r}_{z'x}}{\mathbf{r}_{zy}^2 \mathbf{r}_{z'x}^2} - \left(1 + \frac{z}{z_1} + \frac{z^2}{2z_1^2} \right) \frac{\mathbf{r}_{zx} \cdot \mathbf{r}_{z'x}}{\mathbf{r}_{zx}^2 \mathbf{r}_{z'x}^2} \right] + c.c., \quad (57)$$

with $\bar{Q}_{R2}^2 = (1 - z_1 - z)(z_1 + z)Q^2$ and the CGC correlator

$$\Xi_{\text{NLO},1}(\mathbf{x}_\perp, \mathbf{y}_\perp, \mathbf{z}_\perp, \mathbf{z}'_\perp) = \frac{N_c}{2} \langle 1 - D_{yz'} - D_{xz}D_{zy} + D_{zz'}D_{xz} \rangle - \frac{1}{2N_c} \langle 1 - D_{xy} - D_{yz'} + D_{xz'} \rangle. \quad (58)$$

As for the NLO-4 term, we aim at extracting the LP contribution out of this expression. We also change the variables to $\mathbf{B}_\perp = z_1\mathbf{x}_\perp + (1 - z_1)\mathbf{y}_\perp$ and $\mathbf{r}_{xy} = \mathbf{x}_\perp - \mathbf{y}_\perp$.

We look for a gluon jet in the target fragmentation region with $z \sim \mathbf{P}_\perp^2/Q^2$. Defining $\mathbf{L}_\perp = z_1\mathbf{P}_\perp/z$ such that $L_\perp \sim Q^2/P_\perp$, we have the hierarchy $L_\perp \gg Q \gg P_\perp$ such that $r_{z'} \ll r_{xy} \ll r_{zB}$ from the phases. With this hierarchy of transverse distances in mind, we first simplify the color structure using $\mathbf{z}'_\perp = \mathbf{x}_\perp$

$$\Xi_{\text{NLO},1}(\mathbf{x}_\perp, \mathbf{y}_\perp, \mathbf{z}_\perp, \mathbf{z}'_\perp) \approx \frac{N_c}{2} \langle 1 - D_{yx} - D_{xz}D_{zy} + D_{zx}D_{xz} \rangle - \frac{1}{2N_c} \langle 2 - D_{xy} - D_{yx} \rangle, \quad (59)$$

and we further expand it around \mathbf{B}_\perp up to the first order in \mathbf{r}_{xy} as for the NLO-4 color structure in the previous subsection:

$$\Re\epsilon(\Xi_{\text{NLO},1}(\mathbf{x}_\perp, \mathbf{y}_\perp, \mathbf{z}_\perp, \mathbf{z}'_\perp)) = \mathbf{r}_{xy}^i \frac{N_c}{2} \Re\epsilon \left\langle \frac{1}{N_c^2} \text{Tr}(V_B V_z^\dagger) \text{Tr}(V_z \partial^i V_B^\dagger) \right\rangle + \mathcal{O}(r_{xy}^2) \quad (60)$$

$$= \mathbf{r}_{xy}^i \frac{C_F}{2} \int d^2\mathbf{q}_\perp e^{-i\mathbf{q}_\perp \cdot \mathbf{r}_{zB}} (i\mathbf{q}_\perp^i) \mathcal{D}_A(x, \mathbf{q}_\perp). \quad (61)$$

The quantity inside the big square bracket in Eq. (57) is identical, up to an overall minus sign, to Eq. (45). However, since the expansion of the CGC correlator starts at the order $\mathcal{O}(r_{xy})$, it is sufficient to truncate Eq. (45) up to the order one in $\mathcal{O}(r_{xy})$ and the order zero in z . We thus get

$$\begin{aligned} F_{UU,L}^{\text{NLO},1,\text{LP}} &= \frac{\alpha_s N_c}{8\pi^7} \int_{\mathbf{B}_\perp, \mathbf{r}_{xy}, \mathbf{z}_\perp, \mathbf{z}'_\perp} e^{-i\mathbf{P}_\perp \cdot \mathbf{r}_{zB}} C_F \int_{\mathbf{q}_\perp} e^{-i\mathbf{q}_\perp \cdot \mathbf{r}_{zB}} (i\mathbf{q}_\perp^k) \mathcal{D}_A(x, \mathbf{q}_\perp) \\ &\times \int_0^1 \frac{dz}{z^2} \int_0^1 dz_1 e^{i\frac{z_1}{z} \mathbf{P}_\perp \cdot \mathbf{r}_{z'B}} z_1^3 (1 - z_1)^2 Q^4 K_0(\bar{Q}_{R2} r_{zB}) \mathbf{r}_{xy}^k K_0(Q X_R) \frac{\mathbf{r}_{z'B}^i \mathbf{r}_{xy}^j}{\mathbf{r}_{z'B}^2 \mathbf{r}_{zB}^2} \left[\delta^{ij} - \frac{2\mathbf{r}_{zB}^i \mathbf{r}_{zB}^j}{\mathbf{r}_{zB}^2} \right] + c.c. \\ &= \frac{\alpha_s N_c C_F Q^2}{\pi^5} \int_0^1 \frac{dz}{z} \int_0^1 dz_1 \int_{\mathbf{B}_\perp, \mathbf{q}_\perp} \mathcal{D}_A(x, \mathbf{q}_\perp) z_1 (1 - z_1) \frac{(-\mathbf{q}_\perp^k \mathbf{P}_\perp^i)}{\mathbf{P}_\perp^2} \mathcal{H}_{\text{NLO},1}^{ik} + c.c., \end{aligned} \quad (62)$$

with

$$\mathcal{H}_{\text{NLO},1}^{ik} = \int \frac{d^2\mathbf{r}_{xy}}{(2\pi)} \frac{d^2\mathbf{r}_{zB}}{(2\pi)} e^{-i(\mathbf{P}_\perp + \mathbf{q}_\perp) \cdot \mathbf{r}_{zB}} \frac{\mathbf{r}_{xy}^k \mathbf{r}_{xy}^j}{\mathbf{r}_{zB}^2} \left[\delta^{ij} - 2 \frac{\mathbf{r}_{zB}^i \mathbf{r}_{zB}^j}{\mathbf{r}_{zB}^2} \right] \bar{Q}_1^2 K_0(\bar{Q}_1 r_{xy}) K_0\left(\bar{Q}_1 \sqrt{\mathbf{r}_{xy}^2 + \omega \mathbf{r}_{zB}^2}\right) \quad (63)$$

$$\begin{aligned} &= \frac{1}{12} \left(\delta^{ik} - \frac{2(\mathbf{P}_\perp + \mathbf{q}_\perp)^i (\mathbf{P}_\perp + \mathbf{q}_\perp)^k}{(\mathbf{P}_\perp + \mathbf{q}_\perp)^2} \right) \left[-\frac{1}{\bar{Q}_1^2} + \frac{3\omega}{(\mathbf{P}_\perp + \mathbf{q}_\perp)^2} + \frac{6\omega^2 \bar{Q}_1^2}{(\mathbf{P}_\perp + \mathbf{q}_\perp)^4} \right. \\ &\left. - \frac{6\omega^2 \bar{Q}_1^2 ((\mathbf{P}_\perp + \mathbf{q}_\perp)^2 + \omega \bar{Q}_1^2)}{(\mathbf{P}_\perp + \mathbf{q}_\perp)^6} \ln \left(1 + \frac{(\mathbf{P}_\perp + \mathbf{q}_\perp)^2}{\omega \bar{Q}_1^2} \right) \right]. \end{aligned} \quad (64)$$

Integrating over z_1 and z between z_0 and 1 yields (we also make the change of variable $\mathbf{q}_\perp \rightarrow -\mathbf{q}_\perp$)

$$F_{UU,L}^{\text{NLO},1,\text{LP}} = \frac{\alpha_s N_c C_F}{6\pi^5} \int_{\mathbf{B}_\perp, \mathbf{q}_\perp} \mathcal{D}_A(x, \mathbf{q}_\perp) \frac{\mathbf{q}_\perp^k \mathbf{P}_\perp^i}{\mathbf{P}_\perp^2} \left(\delta^{ik} - \frac{2(\mathbf{P}_\perp - \mathbf{q}_\perp)^i (\mathbf{P}_\perp - \mathbf{q}_\perp)^k}{(\mathbf{P}_\perp - \mathbf{q}_\perp)^2} \right) \left[\frac{5}{6} - \ln \left(\frac{(\mathbf{P}_\perp - \mathbf{q}_\perp)^2}{z_0 Q^2} \right) \right] \quad (65)$$

$$= \frac{\alpha_s N_c C_F}{6\pi^5} \int_{\mathbf{B}_\perp, \mathbf{q}_\perp} \mathcal{D}_A(x, \mathbf{q}_\perp) \left(1 - \frac{2(\mathbf{P}_\perp \cdot (\mathbf{P}_\perp - \mathbf{q}_\perp))^2}{\mathbf{P}_\perp^2 (\mathbf{P}_\perp - \mathbf{q}_\perp)^2} + \frac{\mathbf{P}_\perp \cdot (\mathbf{P}_\perp - \mathbf{q}_\perp)}{\mathbf{P}_\perp^2} \right) \left[\frac{5}{6} - \ln \left(\frac{(\mathbf{P}_\perp - \mathbf{q}_\perp)^2}{z_0 Q^2} \right) \right]. \quad (66)$$

The NLO-0+NLO-3 contributions

We finally consider the diagrams where the gluon sourcing the measured jet does not interact with the shockwave. At the cross-section level, they contribute to $F_{UU,L}$ as (see Eqs. (3.70)-(3.71) in [80])

$$F_{UU,L}^{\text{NLO0}} = \frac{(-\alpha_s)C_F N_c Q^4}{4\pi^7} \int_{\mathbf{x}_\perp, \mathbf{y}_\perp, \mathbf{x}'_\perp} e^{-i\mathbf{P}_\perp \cdot \mathbf{r}_{xx'}} \int_0^1 \frac{dz}{z} \int_0^{1-z} \frac{dz_1}{z^2} e^{-i\frac{z_1}{z}\mathbf{P}_\perp \cdot \mathbf{r}_{xx'}} K_0(\bar{Q}_{R2} r_{x'y}) K_0(\bar{Q}_{R2} r_{xy}) \ln \left(\frac{Q^2 \mathbf{r}_{xx'}^2 R^2 z_1^2}{c_0^2} \right) \\ \times \Re [\Xi_{\text{LO}}(\mathbf{x}_\perp, \mathbf{y}_\perp, \mathbf{x}'_\perp)] (1 - z_1 - z)^2 (z_1 + z)^2 \left(z_1(z_1 + z) + \frac{z^2}{2} \right), \quad (67)$$

for the NLO-0 contribution adapted with the jet definition of [37] and

$$F_{UU,L}^{\text{NLO3}} = \frac{\alpha_s N_c Q^4}{4\pi^8} \int_{\mathbf{x}_\perp, \mathbf{x}'_\perp, \mathbf{y}_\perp, \mathbf{y}'_\perp} e^{-i\mathbf{P}_\perp \cdot \mathbf{r}_{xy}} \int_0^1 \frac{dz}{z} \int_0^{1-z} \frac{dz_1}{z^2} e^{-i\frac{P_\perp}{z} \cdot ((1-z_1)\mathbf{r}_{yy'} + z_1\mathbf{r}_{xx'})} K_0(\bar{Q}_1 r_{xy}) K_0(\bar{Q}_{R2} r_{x'y'}) \\ \times \Re [\Xi_{\text{NLO,3}}(\mathbf{x}_\perp, \mathbf{y}_\perp; \mathbf{x}'_\perp, \mathbf{y}'_\perp)] z_1(1 - z_1)(z_1 + z)(1 - z_1 - z) \left(z_1(1 - z_1 - z) + \frac{z(1 - z)}{2} \right) \frac{\mathbf{r}_{yy'} \cdot \mathbf{r}_{xx'}}{\mathbf{r}_{yy'}^2 \mathbf{r}_{xx'}^2}, \quad (68)$$

for the NLO-3 one. For this jet definition depending on the radius parameter R (assumed to be $\ll 1$), two particles are clustered within the same jet provided $M_{ij}^2/(z_i z_j Q^2) \leq R^2$, with M_{ij} the invariant mass of the pair and $z_i = k_i \cdot P/(P \cdot q)$. In practice, it amounts to changing the argument in the logarithm in Eq. (67) from $P_\perp^2 \mathbf{r}_{xx'}^2 R^2 z_1^2/(z_g^2 c_0^2)$ as shown in [80] to $Q^2 \mathbf{r}_{xx'}^2 R^2 z_1^2/c_0^2$ where $c_0 = 2e^{-\gamma_E}$. As we shall see, the LP gluon jet contribution does not depend on R at our perturbative order, meaning that it is not sensitive to the singularity arising when the integrated quark becomes collinear to the measured gluon. Nevertheless, we expect the jet definition proposed in [37] to play an important role at NNLO in the CGC, as observed in the transversely polarised photon case at NLO where it guarantees that TMD factorisation both in the current and target fragmentation region is preserved by quantum corrections.

In these expressions Eqs. (67)-(68), the CGC correlators are defined as

$$\Xi_{\text{LO}}(\mathbf{x}_\perp, \mathbf{y}_\perp, \mathbf{x}'_\perp) = \langle D_{xx'} - D_{xy} - D_{yx'} + 1 \rangle, \quad (69)$$

$$\Xi_{\text{NLO,3}}(\mathbf{x}_\perp, \mathbf{y}_\perp, \mathbf{x}'_\perp, \mathbf{y}'_\perp) = \frac{N_c}{2} \langle 1 - D_{xy} - D_{y'x'} + D_{xy} D_{y'x'} \rangle - \frac{1}{2N_c} \langle 1 - D_{xy} - D_{y'x'} + Q_{xy;y'x'} \rangle. \quad (70)$$

with the quadrupole $Q_{xy;y'x'} = \frac{1}{N_c} \text{Tr} [V(\mathbf{x}_\perp) V^\dagger(\mathbf{y}_\perp) V(\mathbf{y}'_\perp) V^\dagger(\mathbf{x}'_\perp)]$. The leading power term of these two expressions can be obtained by considering the regime $z \sim P_\perp^2/Q^2$ such that the phases

$$e^{-i\frac{z_1}{z}\mathbf{P}_\perp \cdot \mathbf{r}_{xx'}}, \quad e^{-i\frac{P_\perp}{z} \cdot ((1-z_1)\mathbf{r}_{yy'} + z_1\mathbf{r}_{xx'})}, \quad (71)$$

dominate and therefore impose $\mathbf{r}_{xx'} = 0$, $\mathbf{r}_{yy'} = 0$, i.e. $\mathbf{x}_\perp = \mathbf{x}'_\perp$ and $\mathbf{y}_\perp = \mathbf{y}'_\perp$. With these identifications, the CGC correlators simplify

$$\Re [\Xi_{\text{LO}}] = 2\Re(1 - \langle D_{xy} \rangle) \quad (72)$$

$$= 2\Re \int d^2 \mathbf{q}_\perp (1 - e^{i\mathbf{q}_\perp \cdot \mathbf{r}_{xy}}) \mathcal{D}_F(x, \mathbf{q}_\perp), \quad (73)$$

$$\Re [\Xi_{\text{NLO3}}] = 2C_F \Re(1 - D_{xy}) + \frac{N_c}{2} \Re(\langle D_{xy} D_{yx} \rangle - 1) \quad (74)$$

$$= 2C_F \Re \int d^2 \mathbf{q}_\perp (1 - e^{i\mathbf{q}_\perp \cdot \mathbf{r}_{xy}}) \mathcal{D}_F(x, \mathbf{q}_\perp) + C_F \Re \int d^2 \mathbf{q}_\perp (e^{i\mathbf{q}_\perp \cdot \mathbf{r}_{xy}} - 1) \mathcal{D}_A(x, \mathbf{q}_\perp). \quad (75)$$

Let us first consider the contribution depending on the gluon-gluon dipole $\mathcal{D}_A(x, \mathbf{q}_\perp)$. The latter only comes from $F_{UU,L}^{\text{NLO3}}$. Using

$$\int \frac{d^2 \mathbf{r}_{xx'}}{(2\pi)} \int \frac{d^2 \mathbf{r}_{yy'}}{(2\pi)} e^{-i\frac{P_\perp}{z} \cdot ((1-z_1)\mathbf{r}_{yy'} + z_1\mathbf{r}_{xx'})} \frac{\mathbf{r}_{yy'} \cdot \mathbf{r}_{xx'}}{\mathbf{r}_{yy'}^2 \mathbf{r}_{xx'}^2} = -\frac{z^2}{z_1(1 - z_1)} \frac{1}{\mathbf{P}_\perp^2}, \quad (76)$$

we get

$$F_{UU,L}^{\text{NLO3}}|_A \approx \frac{\alpha_s C_F N_c Q^4}{\pi^6 \mathbf{P}_\perp^2} \int_{\mathbf{B}_\perp, \mathbf{q}_\perp} \mathcal{D}_A(x, \mathbf{q}_\perp) \int d^2 \mathbf{r}_{xy} (1 - e^{i\mathbf{q}_\perp \cdot \mathbf{r}_{xy}}) e^{-i\mathbf{P}_\perp \cdot \mathbf{r}_{xy}} \int_{z_0}^{P_\perp^2/Q^2} \frac{dz}{z} \int_0^1 dz_1 z_1^2 (1 - z_1)^2 K_0^2(\bar{Q}_1 r_{xy}). \quad (77)$$

The upper boundary of the z integral follow from the approximation $z \lesssim P_\perp^2/Q^2$ used to simplify the expressions for the NLO,0 and NLO,3 terms. The lower cut-off z_0 regulates the $z \rightarrow 0$ logarithmic divergence.

For the contribution depending on the $q\bar{q}$ dipole $\mathcal{D}_F(x, \mathbf{q}_\perp)$, coming both from NLO-0 and NLO-3, we have

$$F_{UU,L}^{\text{NLO3}}|_F + F_{UU,L}^{\text{NLO0}}|_F \approx \frac{2\alpha_s C_F N_c Q^4}{\pi^6 \mathbf{P}_\perp^2} \int_{\mathbf{B}_\perp, \mathbf{q}_\perp} \mathcal{D}_F(x, \mathbf{q}_\perp) \int d^2 \mathbf{r}_{xy} (1 - e^{i\mathbf{q}_\perp \cdot \mathbf{r}_{xy}}) (1 - e^{-i\mathbf{P}_\perp \cdot \mathbf{r}_{xy}}) \\ \times \int_{z_0}^{P_\perp^2/Q^2} \frac{dz}{z} \int_0^1 dz_1 z_1^2 (1 - z_1)^2 K_0^2(\bar{Q}_1 r_{xy}). \quad (78)$$

The K_0 Bessel function imposes that $r_{xy} \lesssim 1/\bar{Q}_1 \ll 1/P_\perp, 1/q_\perp$. Therefore, one can expand the remaining phases up to second order in r_{xy} . By rotational invariance, the piece depending on $\mathcal{D}_F(x, \mathbf{q}_\perp)$ vanishes since it depends on $\mathbf{q}_\perp \cdot \mathbf{P}_\perp$ only. For the piece depending on $\mathcal{D}_A(x, \mathbf{q}_\perp)$, we use

$$\int \frac{d^2 \mathbf{r}_{xy}}{(2\pi)^2} \mathbf{r}_{xy}^2 K_0^2(\bar{Q}_1 r_{xy}) = \frac{1}{3\bar{Q}_1^4}, \quad (79)$$

and we eventually get

$$F_{UU,L}^{\text{NLO0+3,LP}} = \frac{\alpha_s N_c C_F}{6\pi^5} \frac{1}{P_\perp^2} \int_{z_0}^{P_\perp^2/Q^2} \frac{dz}{z} \int_{\mathbf{B}_\perp, \mathbf{q}_\perp} q_\perp^2 \mathcal{D}_A(x, \mathbf{q}_\perp). \quad (80)$$

This LP contribution suffers several logarithmic divergences which are regulated by physical scales. For $z \rightarrow 0$, we have introduced a lower cut-off z_0 , which is physically determined by imposing the gluon being on-shell, $2k_g^+ k_g^- = P_\perp^2$, and the condition $k_g^- \leq P^-$ from minus momentum conservation. Resolving this inequality with $k_g^+ = zq^+$ yields $z \geq x_{\text{Bj}} P_\perp^2/Q^2$. We shall then use $z_0 = x P_\perp^2/Q^2$. The integral over \mathbf{q}_\perp is also divergence for $q_\perp \rightarrow \infty$, since typically $\mathcal{D}_A(x, \mathbf{q}_\perp) \propto 1/q_\perp^4$ at large q_\perp . Our derivation sets the natural scale Q^2 at which one should cut the \mathbf{q}_\perp integration, since we have performed the expansion for $1/\bar{Q}_1 \ll 1/q_\perp$.

Final result for the NLO gluon-jet contribution at leading power

Adding all leading power contributions, we get

$$F_{UU,L}^{\text{NLO,LP-g}} = \frac{\alpha_s C_F N_c}{6\pi^5} \int_{\mathbf{B}_\perp, \mathbf{q}_\perp} \mathcal{D}_A(x, \mathbf{q}_\perp) \left\{ \ln \left(\frac{1}{x} \right) \frac{q_\perp^2}{P_\perp^2} - 1 - \frac{(\mathbf{P}_\perp - \mathbf{q}_\perp)^2 - q_\perp^2}{2P_\perp^2} \ln \left(\frac{(\mathbf{P}_\perp - \mathbf{q}_\perp)^2}{P_\perp^2} \right) \right. \\ \left. + \left(1 - \frac{2(\mathbf{P}_\perp \cdot (\mathbf{P}_\perp - \mathbf{q}_\perp))^2}{P_\perp^2 (\mathbf{P}_\perp - \mathbf{q}_\perp)^2} \right) \frac{(\mathbf{P}_\perp - \mathbf{q}_\perp)^2}{P_\perp^2 - (\mathbf{P}_\perp - \mathbf{q}_\perp)^2} \ln \left(\frac{(\mathbf{P}_\perp - \mathbf{q}_\perp)^2}{P_\perp^2} \right) \right\}. \quad (81)$$

The explicit logarithmic dependence upon x fully comes from Eq. (80), where $z_0 = x P_\perp^2/Q^2$ has been used. In the dilute limit $P_\perp \gg q_\perp$, we have

$$F_{UU,L}^{\text{NLO,LP-g}} = \frac{\alpha_s C_F}{6\pi^5} \left[N_c \ln \left(\frac{1}{x} \right) + \frac{(-11)N_c}{6} \right] \frac{1}{P_\perp^2} \int_{\mathbf{B}_\perp, \mathbf{q}_\perp} q_\perp^2 \mathcal{D}_A(x, \mathbf{q}_\perp) \Theta(P_\perp^2 - q_\perp^2) \quad (82)$$

$$= \frac{\alpha_s}{3\pi} \times \frac{\alpha_s}{2\pi^2} \frac{1}{P_\perp^2} \int_x^1 d\xi P_{gg}(\xi) \frac{x}{\xi} G \left(\frac{x}{\xi}, P_\perp^2 \right), \quad (83)$$

with

$$P_{gg}(\xi) = \frac{2N_c [1 - \xi(1 - \xi)]^2}{\xi(1 - \xi)_+}, \quad xG(x, P_\perp^2) = \frac{C_F}{2\pi^2 \alpha_s} \int_{\mathbf{B}_\perp, \mathbf{q}_\perp} q_\perp^2 \mathcal{D}_A(x, \mathbf{q}_\perp) \Theta(P_\perp^2 - q_\perp^2). \quad (84)$$

In the expression for P_{gg} , the plus prescription is defined by

$$\int_x^1 d\xi \frac{f(\xi)}{(1 - \xi)_+} = \int_x^1 d\xi \left[\frac{f(\xi) - f(1)}{1 - \xi} \right], \quad (85)$$

for any function $f(\xi)$ with a well defined limit as $\xi \rightarrow 1$. In the second line of Eq. (83), we have recognized in the numerical factor $2N_c \ln(1/z_0) - 11N_c/3$ the integral of the $g \rightarrow gg$ splitting function $P_{gg}(\xi)$ when $z_0 = x\mathbf{P}_\perp^2/Q^2$. We have also set the longitudinal scale of the gluon PDF to x/ξ to make manifest that the dilute limit corresponds to a single $g \rightarrow gg$ DGLAP step with an incoming gluon from the target wave-function. Strictly speaking, the exact x value of the gluon PDF is not under controlled in our CGC calculation; its determination requires including some sub-eikonal corrections [120–122] as discussed in [123–125] in the context of inclusive DIS and the exclusive Compton process and [126, 127] in the context of the matching between the CGC effective theory and the high-twist formalism.

Finally, the overall factor $\alpha_s/(3\pi)$ in Eq. (83) is the hard factor for the $\gamma_L^* + g$ channel in agreement with the Altarelli-Martinelli identity discussed in section A of this Supplemental Material.
